OFFPRINTS FROM RADON AND ITS DECAY PRODUCTS IN INDOOR AIR
Edited by William W. Nazaroff and Anthony V. Nero, Jr.

2

Soil as a Source of Indoor Radon: Generation, Migration, and Entry

WILLIAM W. NAZAROFF
Environmental Engineering Science, California Institute of Technology, Pasadena, California
Indoor Environment Program, Lawrence Berkeley Laboratory, University of California, Berkeley, California

BARBARA A. MOED and RICHARD G. SEXTRO
Indoor Environment Program, Lawrence Berkeley Laboratory, University of California, Berkeley, California

1 INTRODUCTION

Soil and rock are the source of most radon to which people are exposed. In fact, the only other sources of significance are building materials, and even these generate radon because of radium that originated in the earth (or to a small degree from predecessor radioisotopes that originated in the earth themselves). In discussing radon sources, then, it is common and convenient to distinguish not only among the materials that contain the radium that leads to indoor radon, but also among the agents and pathways by which radon enters. When we speak of soil as the source of indoor radon, we implicitly mean that portion of the total indoor radon concentration which originates in the earthen material underlying the structure and moves directly through the building substructure and into the indoor air. That movement is generally restricted to distances of several meters or less and must occur within several half-lives of radon, i.e., within a few weeks.

The other agents by which radon generated in the soil may enter indoor air are potable water (discussed in Chapter 4) and outdoor air and natural gas (discussed in Chapter 1). For countries in which high indoor radon levels are common, including Canada, the United States, and Sweden, there is growing evidence that the source of most radon at levels of concern in indoor air is the underlying soil from which radon directly enters the building substructure by a combination of convective and diffusive transport. Such evidence may be grouped into three categories: (i) efforts to account for indoor radon concentrations by balancing rates of entry

and removal (1, 2), (ii) remedial measures taken to lower high indoor radon concentrations (3–5), and (iii) theoretical studies of radon migration from soil into buildings (6, 7).

An understanding of the sources and transport processes accounting for radon in indoor air is of considerable importance. Radon levels may be unacceptably high in a substantial proportion of the housing stock in developed countries. In the United States, for example, it has been estimated that one to four million homes have radon concentrations exceeding recently recommended guidelines (8). Furthermore, of the two major factors that determine indoor concentrations—the radon entry rate and the ventilation rate—the entry rate appears to be more variable and hence the more important factor in determining which houses have high levels. Thus, identifying houses with high levels, designing optimal control measures, and predicting the impact of changes in building construction practice on indoor radon concentrations—all depend on knowledge of radon sources.

This chapter is concerned extensively with the transport mechanisms by which radon migrates in soil air and through building substructures. The discussion necessitates a summary of some important characteristics of soil: grain size, permeability, porosity, and moisture content. The mechanisms of radon generation in soil and entry into soil pore space are described. Then some relevant features of building construction and operation that relate to radon entry are discussed. Of particular importance are substructure design, the location and size of substructure penetrations, and operations, such as the use of a fireplace, that may lead to a lowering of the pressure in the structure relative to the outdoors. The physics of radon migration in soil is discussed, including the mechanisms that generate pressure gradients in the soil and lead to convective transport of radon. The relationship between indoor radon concentration and air-exchange rate is explored. Understanding this relationship is necessary to properly interpret the results of field measurements and to accurately predict the effect of changes in building operation on the indoor concentration. The final section illustrates one application of a detailed understanding of soil as a source of indoor radon: identification of areas for which high indoor radon concentrations are likely on the basis of geological and geographical data collected for other purposes.

The focus of the present discussion is on the most abundant radon isotope, ^{222}Rn, and on the building practices used for single-family dwellings in the United States. Thoron (^{220}Rn), the other radon isotope of some importance, is discussed to a lesser degree. Although on average it is generated at the same rate in soil as ^{222}Rn, its much shorter half-life leads to a much shorter transport range and generally lower concentrations indoors. The discussion is, for the most part, sufficiently general that the extension to other building types follows once the key building characteristics are identified. Control techniques for preventing the direct entry of radon from soil are discussed extensively in Chapter 10 and consequently are not treated here.

A schematic representation of the key elements of soil as a source of indoor radon is presented in Figure 2.1. It is useful to distinguish two main concepts.

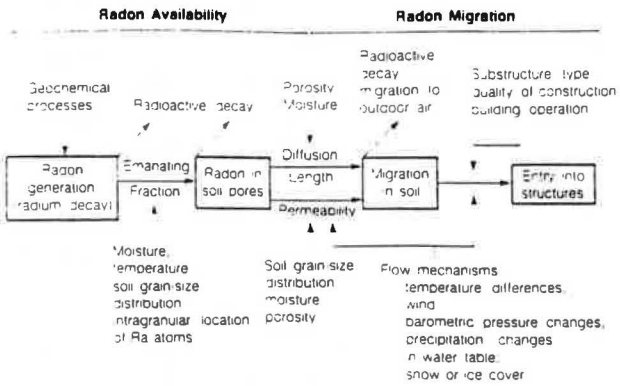

Figure 2.1. Schematic representation of radon production and migration in soil and its entry into buildings.

"Radon availability" identifies the factors that influence the concentration of radon in soil air in the absence of structures. These parameters determine the source potential of the soil. "Radon migration" groups the factors that determine the movement of radon from the soil air into buildings. This element depends on both soil and building-related factors. Both concepts contribute to the process by which soil serves as a source of indoor radon. They combine in a manner that is roughly multiplicative: soil is a small source of indoor radon if either the rate of generation of radon in the soil pores or the rate of transport of radon from the soil into the building is small.

In Figure 2.1, the boxes represent the major states of radon from its generation in soil to its entry into a building; labels on horizontal arrows indicate a characteristic of the soil that is a measure of how readily radon moves from one state to the next; labels on vertical arrows indicate parameters and processes that significantly influence the rate or transition from one state to another. Labels on diagonal arrows indicate paths by which radon generated in soil may fail to enter a building. Among many features of this representation, one may note that moisture plays a role at several steps in the process.

2 PHYSICAL CHARACTERISTICS OF SOIL

As might be expected, the physical characteristics of a soil play key roles in determining the radon concentration in nearby buildings. Many of these characteristics have been widely investigated for other purposes by civil engineers (9, 10), agronomists (11), petroleum engineers (12–14), and groundwater hydrodynamicists. Consequently, it is instructive to briefly review the information from these fields that is relevant to indoor radon. Important factors relating to radon production in soil are outside the scope of these fields and are discussed in Section 3.

2.1 Grain-Size Distribution, Porosity, and Moisture Content

Soils have two major volume fractions. The solid fraction consists mainly of mineral grains of a wide range of sizes, and also includes a small amount of organic matter. The void fraction consists of liquid, usually water, and gas. The gas is generally similar in composition to air. The void fraction is also known as the soil porosity, and the volume fraction of water is often called the moisture content. A soil is saturated when the moisture content equals the porosity.

Soils are classified according to the size distribution of the solid grains, with the major divisions being clay, silt, and sand. Characteristic particle sizes for each class are given in Table 2.1. Grains larger than sand and up to 15 cm in diameter are classified as gravel. In contrast to the larger particles, which are formed by mechanical weathering, clays are formed by chemical processes. Because of their small size and active surfaces, they may interact in a complex manner with other grains and with water. Consequently, they exhibit macroscopic properties, particularly sorption of radioisotopes and interaction with water, that are quite different than those of silts and sands.

Apart from this distinction in the formation process between clays and other soil types, the physical characteristics of soil pertaining to fluid flow vary widely with grain size distribution. However, attempts to predict these characteristics for a particular soil on the basis of grain size distribution have not been very successful. Discussions of such efforts may be found in the literature (12–15). Here, we present some representative data and simple analytical results as a basis for making numerical estimates of radon migration rates through soil.

Soil porosities are commonly in the vicinity of 0.5. By comparison, uniformly sized spheres have a porosity between 0.26 (close packing) and 0.48 (open packing). Because of the greater tendency for small particles to "bridge," clays tend to have higher porosities than sands. Poorly sorted soils, that is, having a wide range of grain sizes, may have porosities of 0.3 or less.

The pore space within soils may be thought of, paradoxically, as both continuous and discrete: large pores are connected by narrower channels. The pore space has two major components: the "textural" pore space, always present, which results from the random packing of the soil particles; and "structural" pore space, present only in well-aggregated soils, which exists between the soil aggregates. Transient aggregates may form owing to cracking upon drying in soils containing a high percentage of clay-sized particles. Long-lived aggregates, which withstand

TABLE 2.1 Representative Values of Physical Characteristics of Soil

Type	Grain size (μm)	Porosity	Field capacity, saturation (%)[a]	Wilting point, saturation (%)[a]
Sand	60–2000	0.4	15	5
Silt	2–60	0.5	58	10
Clay	<2	0.6	68	48

[a]A saturation of 100% means that the entire pore volume is filled with water.

Source: Ref. 17.

wetting cycles, tend to form in soils containing much colloidal and organic material (16).

The moisture content of a soil not only depends on the grain-size distribution, but may be highly variable over time. A variety of physical effects control the migration of liquid water in the soil pores. These forces form the basis for distinguishing among the components of the liquid phase (11). For our purposes, a classification system with three categories is most useful. The "hygroscopic" component of soil water is adsorbed on the grain surfaces by local electrostatic forces. This component is the most tightly bound and may be retained for relatively long time periods even when the soil is otherwise dry. It is particularly important in clays owing to the small grain size, the polar nature of water molecules, and the crystalline structure of the clay particles. The "capillary" component of soil water is held in small pores and in a film around the particles by surface tension. The most variable component is termed "gravitational" water—that contained in the large pores—which is free to move under the influence of gravity.

Some understanding of the magnitude of these components for different soil types may be gained from the parameters "field capacity" and "wilting point" (17). The field capacity refers to the volume fraction of water in soil after it has been thoroughly wetted, then drained for about 2 days. The wilting point refers to the moisture content at which test plants growing on the soil wilt and do not recover if their leaves are kept in a humid atmosphere overnight. These can be expressed in terms of the saturation percent or volume percent, determined with respect to the pore volume or total volume, respectively. As with porosity, both parameters increase with decreasing particle size. Typical values for the field capacity and for the wilting point are presented in Table 2.1.

Moisture content is a very important factor for radon emanation and migration in soil. For a well-drained soil, the void volume contains water in the smaller pores and air in the larger pores. As discussed in Section 3.2, the capillary water increases the radon emanation fraction by absorbing the recoil energy of the newly formed atom. However, this water does not increase the resistance of the soil to airflow to a great degree since it is the larger pores that make the dominant contribution.

2.2 Permeability

One of the most important physical characteristics of soil pertinent to indoor radon is its permeability, i.e., how readily a fluid—in this case air—may flow through it. Permeability relates the apparent velocity of fluid flow through the soil pores to the pressure gradient. This relationship, described by Darcy's law, is discussed in detail in Section 5.2. Here, our attention is focused on the range of values of soil permeability and the factors that may affect it.

The importance of soil permeability in the study of indoor radon arises from the very broad range of values it assumes: as shown in Figure 2.2, the permeability of common soils in the absence of structural pores may span more than 10 orders of magnitude. We shall see that at the lower end of this range, molecular diffusion

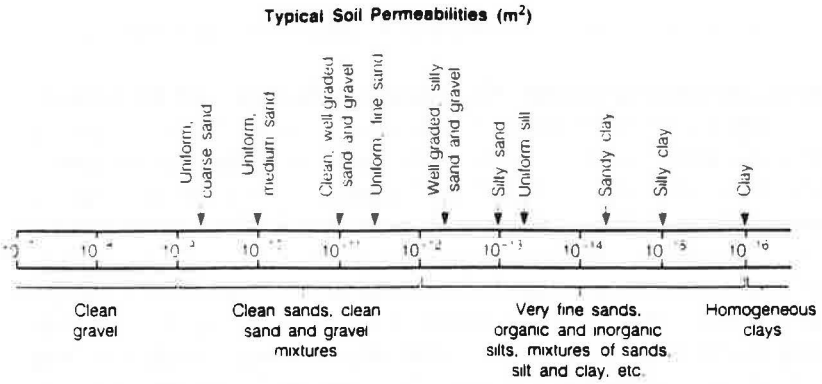

Figure 2.2. Permeability (m^2) of representative soil types. Data from Terzaghi, K., and Peck, R. B. (1967). *Soil Mechanics in Engineering Practice*, 2nd ed., Wiley, New York; Tuma, J. J., and Abdel-Hady, M. (1973). *Engineering Soil Mechanics*, Prentice-Hall, Englewood Cliffs, NJ, p. 102.

becomes the dominant process by which radon migrates through soil near buildings. At the upper end of this range, convective flow is the dominant radon transport mechanism. Since the convective flow rate increases with increasing permeability, and since the radon entry rate increases with convective flow of soil air into the substructure, the potential for radon entry is expected to increase monotonically with permeability for large grained soils. The actual entry rates are influenced by the characteristics of the building shell and the building operation.

Conceptually, permeability is based on the macroscopic properties of soil, i.e., the bulk volume flux of a fluid for a given pressure differential. This bulk property clearly depends on the microscopic characteristics of the soil: the size, shape, number, and orientation of pores, in particular, and the moisture content. Larger-grained soils generally have higher permeabilities: their pores are larger, and consequently the frictional resistance to fluid flow at the surface of the grains is of lesser importance than it is in fine-grained soils. Beyond this qualitative understanding, there has been considerable research toward establishing relationships between physical parameters of a porous medium and its permeability. The approaches have included empirical correlations, simplified physical modeling, and statistical theories. As discussed by Scheidegger (12), probably the most widely accepted approach to linking geometrical properties of a porous medium with its permeability was first developed by Kozeny. His approach was to solve the Navier-Stokes equation, which describes the momentum balance in a fluid, for an assemblage of channels of various cross-sections, but of constant length. When the resulting flow is compared with Darcy's law, the following expression for permeability is obtained:

$$k = \frac{c\epsilon^3}{TS^2} \tag{1}$$

where c is a constant that depends on the pore shape and, theoretically, varies between 0.5 and 0.67; ϵ is the porosity; T is the tortuosity, an empirical factor greater than or equal to 1.0 that accounts for the fact that the flow channels are not straight; and S is the specific surface area. For uniform, spherical particles

$$S = \frac{6(1 - \epsilon)}{d} \tag{2}$$

where d is the particle diameter.

For uniformly sized particles, we see that the permeability varies approximately as the square of the particle diameter. In Table 2.2 we present representative permeabilities for the three main soil types based on this equation. In comparing these results with Figure 2.2, we see that the representative permeabilities show the same general dependence on particle size as indicated by the characteristic data.

The Kozeny theory applies only to a soil completely saturated with the fluid of interest. For the case at hand, this means a soil with a small moisture content. In general, the permeability of soil is dependent on the degree of saturation of the fluid, especially within the large pores. Recognition of this dependence has led to the use of the term "relative permeability," which is defined as the ratio of the effective permeability at a given saturation to the permeability when the saturation is 100% for the fluid of interest (18). Studying variations in relative permeability with percent saturation improves our understanding of the influence of moisture content on the air permeability of soils.

Figure 2.3 shows the relative permeability for air (k_{ra}) and water (k_{rw}) as functions of water saturation for a loamy sand. An important point is illustrated here: for this soil, the value of the air permeability remains roughly constant and equal to that for the soil when dry, until water fills a large fraction, about 42%, of the pore space. For the surface and subsurface samples studied, the percent saturation at field capacity was 43% and 47%, respectively, suggesting that the air permeability, for sandy soils, is not strongly affected by changes in moisture content below the field capacity. As moisture content increases above field capacity, the large pores begin to fill with water, and the reduction in air permeability is large. Other studies have shown that the air permeability at field capacity ranges from 0.6 to 0.8 of that of the dry medium (19, 20).

The influence of moisture content below field capacity on the air permeability is greater for clayey soils than for sandy soils for two reasons: the mean pore size

TABLE 2.2 Representative Permeabilities (k) Based on Kozeny Theory[a]

Soil type	d (μm)	ϵ	S (m^{-1})	k (m^2)
Clay	1	0.6	2×10^6	1×10^{-14}
Silt	20	0.5	2×10^5	1×10^{-12}
Sand	200	0.4	2×10^4	4×10^{-11}

[a] $c = 0.5$; $T = 1/\epsilon$ (117); d = particle diameter; ϵ = porosity; S = specific surface area.

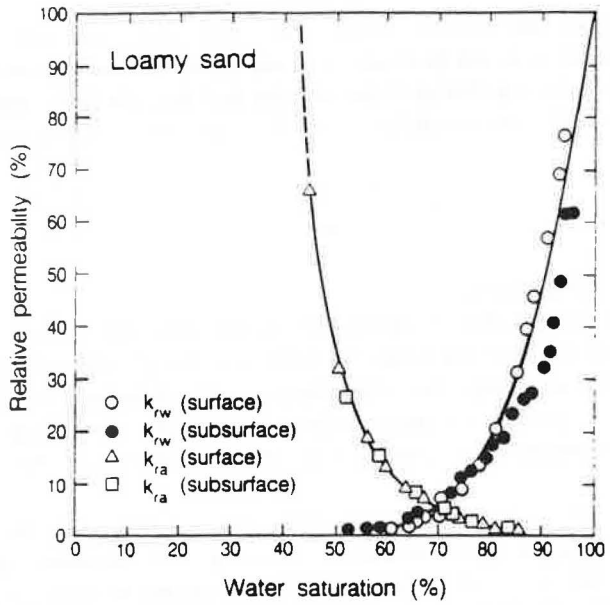

Figure 2.3. Relative permeability of loamy sand for air (k_{ra}) and water (k_{rw}) as a function of water saturation.

is smaller than in sands, so that at field capacity there is a greater tendency for pore blockage in clayey soils; and clayey, or cohesive, soils develop aggregates between which most of the fluid flow occurs (21–23). The formation of aggregates is, as mentioned above, strongly influenced by moisture content.

A further important consideration is the possibility of chemical interactions between soil grains and water. Such interactions tend to retard the flow of water through the soil. Consequently, the apparent intrinsic permeability for water flow through soil may be lower than that for airflow through soil. Since most measurements of the permeability of soil have used water as the fluid, there may be a systematic underestimation in applying these data to the analysis of radon migration in soil.

In addition to the complicating effect of soil moisture, theoretical analyses, such as that due to Kozeny, invariably reflect analyses on a porous medium that is an idealization from even the most regular soil. Undisturbed soils exhibit many complicating features. All soils consist of a distribution of particle sizes, and both the breadth of the distribution and its shape may affect permeability in a way that is not adequately described by the specific surface area. Another factor that may be of particular importance in considering soil as a source of indoor radon is anisotropy in soil permeability. For example, because sedimentary beds are deposited in layers with particles settling under the combined forces of gravity and fluid drag, one might generally expect the permeability of an undisturbed sedimentary soil to be greater in the horizontal than in the vertical direction. One might further expect this effect to be enhanced for platelike clay minerals, as compared to more

rounded sand grains. Directional permeability measurements have been made on samples of water-bearing consolidated soils consisting of sand, silt, and clay. The results showed higher horizontal permeabilities by factors of 1.4–7, depending on the site (24). Similar measurements were made on settled sand and limestone samples. Again, where there were differences, the horizontal permeability was higher, but typically by only 20% for these cases. Differences between horizontal and vertical permeabilities of less than an order of magnitude may not be significant, given the range of permeability values. However, differences of a factor of 1000 have been measured (25). The significance for radon entry is this: a higher permeability in the horizontal than in the vertical direction may lead to a larger volume of soil providing radon for the structure.

Structural pore space, when present, strongly influences the permeability of soil and may impart to soils that are texturally clays and clay loams permeabilities similar to those of coarse sands (26). The presence of biopores—penetrations in the soil due to animal or plant activity—may also increase the permeability of fine- and medium-textured soils to values similar to those associated with coarse-textured soils (27).

Whatever complications exist in assessing the behavior of undisturbed soils from theoretical analyses are amplified in investigating radon entry into buildings. Here the nearby soils have often been disturbed and redistributed during construction, and the roots of landscaping vegetation may increase the local permeability. Nevertheless, these effects may be of secondary importance relative to the very large effect of particle size on permeability. Consequently, simple on-site measurements or relevant data from published sources on soil grain-size distribution or permeability may be of considerable use in strategies and techniques for identifying buildings with high concentrations.

2.3 Diffusivity

Owing to random molecular motions, there is a tendency for a substance to migrate down its concentration gradient in a material. As is discussed in Section 5.1, this tendency is described by Fick's law, which relates a concentration gradient to a flux. The coefficient relating these parameters is termed the molecular diffusivity, or diffusion coefficient. In a porous medium, it is a property of the fluid in the pores, the pore structure, and the diffusing species.

For a porous material there are as many as four ways in which Fick's law may be written, depending on whether one uses bulk or pore volume to determine concentration and bulk or pore area to determine flux density; different diffusion coefficients result, and the symbols and terminology have not become standardized in the literature. The "bulk" diffusion coefficient, herein denoted D, relates the gradient of the interstitial concentration of the diffusing species to the flux density across a *geometric* or *superficial* area. The "effective" or "interstitial" diffusion coefficient, denoted D_e, relates the gradient of the interstitial concentration to the flux density across the *pore* area. (Note that this is equivalent to the coefficient that relates the gradient of the bulk concentration to the flux density across the

geometric area. The fourth possible formulation has, fortunately, not been used.) These coefficients are related by the porosity, ϵ:

$$D = D_v \epsilon \tag{3}$$

The diffusion of radon in soil has been investigated for several purposes. Globally, the movement of radon from soil into the atmosphere appears to be primarily due to molecular diffusion (28). Since little radon is emitted from oceans, it has been used as an atmospheric tracer for continental air masses (29). Another interest in which radon diffusivity in soil arises is uranium exploration: by mapping soil gas concentrations of radon near the surface, one may be able to identify subsurface deposits of soils enriched in uranium (30). Diffusion of radon through soil has recently been investigated in connection with the use of earthen covers to retard the release of radon into the atmosphere from uranium mill-tailings piles (31, 32). Radon diffusion in soil has also been studied in connection with earthquake prediction (33).

The results of several measurements of the radon diffusion coefficient in soil are summarized in Table 2.3. The upper bound is given by the diffusion coefficient of radon in open air (denoted D_o), 1.2×10^{-5} m^2 s^{-1} (34). Typically, the effective diffusion coefficient of radon in soil of low moisture content is 10^{-6} m^2 s^{-1}.

As in the case of permeability, there have been numerous attempts to relate the diffusivity ratio D/D_o to the physical parameters, particularly ϵ, of the porous medium. From work on CO_2 migration in soils, Buckingham (35) proposed the correlation

$$\frac{D}{D_o} = \epsilon^2 \tag{4}$$

Later Penman (36), studying a wide range of porous materials, obtained the correlation

$$\frac{D}{D_o} = 0.66\epsilon \qquad 0.0 < \epsilon < 0.6 \tag{5}$$

Currie (37) discussed other correlations and reported on experiments showing that such correlations must account for the shape of the grains. He concluded that a correlation of the form

$$\frac{D}{D_o} = \gamma \epsilon^{\mu}, \tag{6}$$

where γ and μ are properties of the material, fit data from a wide range of media.

Water plays an important role in influencing the radon diffusion coefficient in soil. In a saturated soil, the radon diffusion coefficient may be reduced to $2 \times$

TABLE 2.3 Effective Diffusion Coefficients for Radon in Soil

Soil description	Ref.	D_e ($m^2 s^{-1}$)	Comments
Mill tailings (2 samples)	32	$(5.4–7.2) \times 10^{-6}$	Moisture content 0.7–1.5% dry weight
Eluvial-detrital granodiorite	38	4.5×10^{-6}	Dry
Silty sandy clay	32	2.7×10^{-6}	Moisture content 1.5% dry weight
		2.5×10^{-7}	Moisture content 10.5% dry weight
		6.0×10^{-8}	Moisture content 17.3% dry weight
Compacted silty sands (12 samples)	31	$(3.0 \pm 1.3) \times 10^{-6}$	Porosity = 0.29–0.36; Saturation = 0.05–0.34
Compacted clayey sands (12 samples)	31	$(3.2 \pm 1.5) \times 10^{-6}$	Porosity = 0.32–0.39; Saturation = 0.09–0.55
Compacted inorganic clays (5 samples)	31	$(2.5 \pm 1.0) \times 10^{-6}$	Porosity = 0.32–0.43; Saturation = 0.06–0.34
Diluvium of metamorphic rocks	38	1.8×10^{-6}	Dry
Eluvial-detrital deposits of granite	38	1.5×10^{-6}	Dry
Loams	38	8×10^{-7}	Dry
Varved clays	38	7×10^{-7}	Dry
Mud	38	5.7×10^{-10}	37% Moisture
Mud	38	2.2×10^{-10}	85% Moisture

10^{-10} m^2 s^{-1} (38). This value is so much lower than that in air that, for practical purposes, we can view the effect of water on the radon diffusion coefficient in soil as blocking a fraction of the available pore space. The results of one study of the radon diffusion coefficient as a function of the fraction of pore space filled with water are presented in Figure 2.4. For low moisture contents, water is predominantly on grain surfaces and in small pores. Since transport through the larger pores dominates, the diffusion coefficient is a weak function of moisture content. As the soil nears saturation, the larger pores become occluded and the rate of reduction in diffusion coefficient with increasing moisture content grows.

Currie (39) investigated the relationship between moisture content of porous materials and the bulk diffusivity of hydrogen. He classified materials according to whether or not the grains had an internal pore structure: sand, for example, constituted a solid particle system, whereas a soil containing much clay was considered a "crumbly" particle system. He found that the behavior of these two types differed, particularly when nearly dry. In this case, the diffusivity depended very slightly on moisture in the crumbly particle system, but strongly on moisture in the solid particle system. He interpreted these data as indicating that the moisture in the crumbly particle system was taken up in the internal pores of the particles and, hence, had little influence on diffusive transport through the sample, which was dominantly through the larger pores. Once the internal pores were saturated, the solid and crumbly particle systems behaved similarly, with the dependence of diffusivity on moisture well represented by

$$\frac{D_w}{D} = \left[\frac{\epsilon_a}{\epsilon}\right]^{\sigma} \tag{7}$$

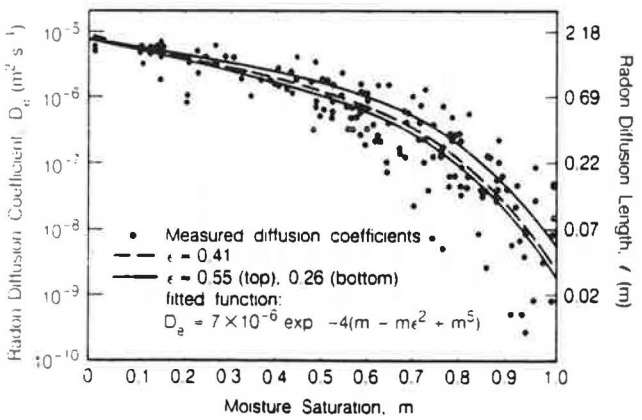

Figure 2.4. Effect of soil moisture content on radon diffusivity. Moisture saturation (m) is the fraction of pore volume filled with water. The porosity is indicated by ϵ. Reproduced from Rogers, V. C., Nielson, K. K., and Kalkwarf, D. R. (1984). Radon attenuation handbook for uranium mill tailings cover design, report NUREG/CR-3533, US Nuclear Regulatory Commission, used by permission.

with σ approximately equal to 4. In this equation D_w is the bulk diffusion coefficient of the wet soil, and ϵ_a is the air-filled porosity (air volume divided by total volume).

The diffusion coefficient for the other isotopes of radon has been observed to be comparable to that for ^{222}Rn.

3 RADON PRODUCTION IN SOIL

This section focuses on the characteristics of soil that influence the rate of radon emanation into the pore air of the soil. We consider two parameters: the radium content and the emanation coefficient.

3.1 Radium Content

The radium content of the soil is typically given as an activity concentration per unit mass. The radium content in these terms is equivalent to the total production rate of radon in the soil, with 1 Bq kg^{-1} of radium yielding radon at a rate of 1 atom kg^{-1} s^{-1}.

Table 2.4 and Figure 2.5 present data on ^{226}Ra and ^{232}Th concentrations in surface soils. The data in Figure 2.5 are based on aerial measurements of ^{214}Bi gamma emissions (40). These data reflect the strength of such emissions from a depth of up to 0.5 m of soil. Two factors may systematically bias these results. First, a fraction of the radon produced in the soil migrates into the atmosphere: hence, the bismuth activity near the surface of a uniform soil is lower than its radium activity. Second, soil bulk density varies (but not proportionately) with moisture content, and gamma attenuation is directly related to density. Consequently, aerial gamma measurements of a given soil are inversely related to its moisture content. The exposure rate above a soil containing 50% water by weight is 36% lower than that above the same soil when dry (41). Since the calibration pads for the aerial detectors contained 20–30% water, the measurements can be in error by up to 20% owing to this effect.

The data in Table 2.4 result from measurements of gamma activity of soil samples collected primarily along U.S. interstate highways (42). The ^{226}Ra content was determined primarily from ^{214}Bi emissions from samples that had been sealed and stored long enough for ^{214}Bi to come to equilibrium with its radium precursor. Data on ^{232}Th, the primordial precursor of ^{220}Rn, reflect gamma emissions from a combination of its decay products. The longest-lived species in the chain from ^{232}Th to ^{220}Rn is ^{228}Ra, with a half-life of 5.7 years, very short in terms of geological time scales. Hence, the ^{232}Th content of a soil is a good indicator of its rate of production of ^{220}Rn.

The radium content of soils tends to reflect the radium content of the rocks from which the soil formed. Table 2.5 summarizes the ^{226}Ra and ^{224}Ra content of rocks. These data are a compilation of over 2500 laboratory-based γ-spectrometric anal-

TABLE 2.4 ^{226}Ra and ^{232}Th Concentrations in Surface Soils

State	No. samples[a]	^{226}Ra (Bq kg^{-1})[b]	^{232}Th (Bq kg^{-1})[b]
Alabama	8	30 (17–52)	28 (13–56)
Alaska	6 (7)	24 (16–34)	32 (7–85)
Arizona	6	35 (9–74)	23 (7–48)
Arkansas	0 (1)		59
California	3	28 (9–48)	20 (11–28)
Colorado	32 (20)	52 (18–126)	48 (4–115)
Delaware	2	43 (41–44)	44
Florida	11 (10)	31 (9–85)	9 (4–14)
Georgia	9	33 (17–59)	41 (10–126)
Idaho	12 (13)	41 (24–59)	44 (16–70)
Illinois	7 (8)	36 (24–44)	36 (18–44)
Indiana	2	39 (37–41)	43 (41–44)
Kansas	6 (4)	36 (13–52)	48 (12–59)
Kentucky	13 (12)	56 (30–155)	44 (33–56)
Louisiana	2	26 (21–31)	24 (22–26)
Maryland	6	27(18–44)	26 (18–32)
Michigan	10	41 (17–74)	21 (9–30)
Mississippi	3	44 (28–59)	41 (30–63)
Missouri	10	41 (11–52)	37 (12–48)
Nevada	6	56 (33–74)	56 (23–111)
New Jersey	24 (23)	32 (9–52)	33 (11–56)
New Mexico	13	56 (27–100)	35 (18–67)
New York	6	31 (18–44)	26 (15–41)
North Carolina	8	29 (18–44)	34 (16–56)
Ohio	12	56 (30–93)	37 (26–56)
Oregon	8 (9)	30 (9–78)	27 (16–56)
Pennsylvania	33	44 (17–89)	41 (14–63)
Tennessee	10 (11)	41 (24–52)	35 (24–56)
Texas	10	33 (20–52)	27 (15–41)
Utah	32 (28)	48 (20–70)	41 (7–85)
Virginia	13	31 (22–41)	32 (16–52)
West Virginia	11	48 (29–59)	52 (41–59)
Wyoming	13 (12)	37 (24–63)	41 (22–67)
All samples	327 (331)	41 (9–155)	36 (4–126)

[a]Where two numbers are given, the one in parentheses applies to ^{232}Th.
[b]Arithmetic mean (range of values in parens).

Source: Ref. 42.

yses reported in English-language publications (43). The radium concentrations within each rock class except the intermediate extrusives were found to be distributed lognormally. Radium contents tended to decrease with silica contents in extrusive and intrusive igneous rocks, with the exception of alkali feldspathoidal rocks, which are rare. The extremely high ^{226}Ra contents listed in the ranges within the chemical sedimentary and shale classes are undoubtedly due to phosphates and black shales, respectively. The mean values for rocks excluding alkali rocks in

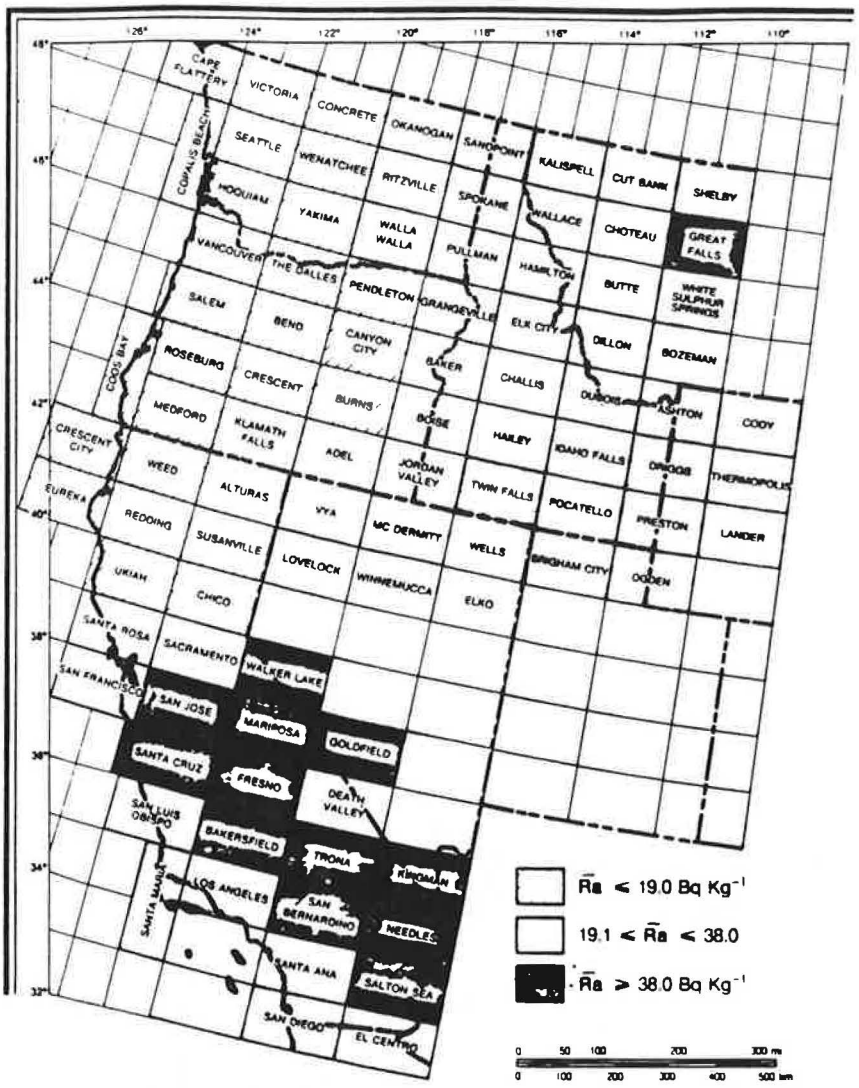

Figure 2.5. Geographical distribution of mean ^{226}Ra content by quadrangle, $\overline{Ra}$, of surface soils for the Western United States. These results are based on an analysis of aerial radiometric data. Reproduced from Ref. 40.

Table 2.5 tend to support the data for soils given in Table 2.4; the ranges suggest that the range of Ra concentrations, even in soils distant from U mining and milling sites, is probably larger than indicated in Table 2.4.

In combination, these studies suggest that surface soils in the United States typically contain 10–100 Bq/kg of both ^{226}Ra and ^{224}Ra.

Values much higher than the range given by these studies have been found in soils near uranium mining areas and mill-tailings piles. For example, Powers et

TABLE 2.5 Radium Concentrations in Rocks

Rock class[b]	Example	No. samples	^{226}Ra (Bq kg^{-1}) Mean[c]	^{226}Ra (Bq kg^{-1}) Range	No. samples	^{228}Ra (Bq kg^{-1})[a] Mean[c]	^{228}Ra (Bq kg^{-1})[a] Range
Acid extrusives	Rhyolite	131	71	10–285	131	91	4–470
Acid intrusives	Granite	569	78	1–372	573	111	0.4–1025
Intermediate extrusives	Andesite	71	26	2–64	71	27	2–113
Intermediate intrusives	Diorite	271	40	1–285	273	49	2–429
Basic extrusives	Basalt	77	11	0.4–41	77	10	0.2–36
Basic intrusives	Gabbro	119	10	0.1–71	110	9	0.1–61
Ultrabasic rocks	Dunite	31	4	0–20	30	6	0–30
Alkali feldspathoidal intermediate extrusives	Phonolite	138	368	24–769	139	543	38–1073
Alkali feldspathoidal intermediate intrusives	Syenite	75	692	4–8930	75	5	2–3560
Alkali basic extrusives	Nephelinite	27	29	6–149	27	36	8–2670
Alkali basic intrusives	Foidite	8	29	5–67	34	8	11–81
Chemical sedimentary rocks[d]	Evaporites	243	45	0.4–335	239	60	0.1–535
Carbonates	Limestone	141	25	0.4–223	131	7	0–45
Detrital sedimentary rocks[e]		412	60	1–992	411	50	0.8–1466
Clay		40	50	14–198	40	35	8–223
Shale		174	73	11–992	174	66	21–158
Sandstone and conglomerate		198	51	1–770	198	39	3–919
Metamorphosed igneous rocks	Gneiss	138	50	1–1835	138	60	0.4–421
Metamorphosed sedimentary rocks	Schist	207	37	1–657	208	49	0.4–368

[a]Because of the short half-lives of ^{228}Ac (6.1 h), ^{228}Th (1.9 y), and ^{224}Ra (3.7 d), one expects ^{224}Ra to be in equilibrium with ^{228}Ra.
[b]Rocks are classified on the bases of whole-rock silica content (acid > intermediate > basic > ultrabasic) and alkali and calcic feldspar mineralogy.
[c]Arithmetic mean.
[d]Includes carbonates.
[e]Includes clay, shale, sandstone, and conglomerates.

Source: Ref. 43.

al. (44) found a range of 15–1700 Bq/kg of ^{226}Ra for 28 samples collected near uranium mining and milling areas in Wyoming, New Mexico, and South Dakota. In Jaduguda, Bihar, India, an area with known deposits of uraniferous materials, ^{226}Ra concentrations of 40–200 Bq/kg were reported (45). Sixty-three samples from Canada collected near the surface of two mill-tailings piles contained a mean ^{226}Ra concentration of 1760 Bq/kg (46).

3.2 Emanation Coefficient

Only a fraction of the radon generated in soil ever leaves the solid grains and enters the pore volume of the soil. This fraction is known as the "emanation coefficient" or, alternatively, "emanating fraction" or "emanating power."

Experimental measurements of the emanation coefficient of rocks and soils have been made by many investigators. These data, summarized in Table 2.6, indicate an approximate range of 0.05–0.7 for soil. We have some understanding of the basic physical processes leading to radon emanation from soil (see Fig. 2.6); however, measured emanation coefficients are considerably higher than predicted by simple physical models.

Conservation of linear momentum dictates that, upon being created by the alpha decay of radium, ^{222}Rn and ^{220}Rn atoms possess kinetic energies of 86 and 103 keV, respectively (47). The newly formed atom travels from its site of generation until its energy is transferred to the host material. The distance traveled depends on the density and composition of the material. The range of ^{222}Rn is 0.02–0.07 μm for common minerals, 0.1 μm for water, and 63 μm in air; the range of ^{220}Rn in air is 83 μm (48).

The emanation coefficient is considered to have three components: direct recoil, indirect recoil, and diffusion. These components arise from the locations of the end points of the path of the recoiling radon atoms. The direct recoil fraction refers to radon atoms that terminate their recoil in the fluid-filled pore space. Atoms that leave the grain in which they were created, traverse a pore, and penetrate another grain form the basis for the indirect-recoil fraction. They must then migrate out of the pocket created by their passage to enter a pore. The diffusion fraction refers to radon atoms that begin and end their recoil within a single grain, then migrate to the pore through molecular diffusion.

Analysis of the emanation process for uniformly distributed radium in undamaged soil grains leads to much lower emanation coefficients than are generally observed. Consider first the maximum recoil fraction. Only radium atoms within the recoil range of the surface generate radon atoms that have any possibility of escaping the grain. Andrews and Wood (49) and Bossus (47) computed the escape probability for radon atoms generated within the recoil range of the surface of a spherical particle and obtained 23.5 and 25%, respectively. If we then consider a spherical particle, with diameter 20 μm (corresponding to a medium-coarse silt), having a radon recoil range of 0.035 μm, this model predicts that only 0.25% of the radon atoms generated in the grain leave it during recoil. An analysis of the

TABLE 2.6 Measurements of ^{222}Rn and ^{220}Rn Emanation Coefficients

Material	No. samples	Moisture content	Isotope	Emanation coef.[a]	Ref.
Rock (crushed)	58	Unknown	^{222}Rn	0.084 ± 0.086 (0.005–0.40)	52
Soil	21	Unknown	^{222}Rn	0.30 ± 0.16 (0.03–0.55)	52
Soil[b]	1	Dried, 105°C, 24 h	^{222}Rn	0.25	50
Soil[c]	1	20% of dry wt	^{222}Rn	0.68	56
		Dried, 200°C, 90 h		0.09	
Soil	1	Air-dry[d]	^{222}Rn	0.41	2
Soil	2	13–20% of dry wt	^{222}Rn	0.27 (0.22–0.32)	92
Soil	1	4% of dry wt	^{222}Rn	0.38 ± 0.08	100
Various soils (Hawaiian)					53
Lava fields		Unknown	^{222}Rn	0.02	
Thin organic soils		Unknown	^{222}Rn	0.55	
Deep agricultural soils		Unknown	^{222}Rn	0.70	
Various soils					118
Sand	7	Unknown	^{222}Rn	0.14 (0.06–0.18)	
Sandy loam	7	Unknown	^{222}Rn	0.21 (0.10–0.36)	
Silty loam	7	Unknown	^{222}Rn	0.24 (0.18–0.40)	

[Heavy] loam	12	Unknown	^{222}Rn	0.20 (0.17–0.23)	
Clay	5	Unknown	^{222}Rn	0.28 (0.18–0.40)	
Various soils (Danish)	70	0–70% of dry wt	^{222}Rn	0.22 ± 0.13 (0.02–0.7)	119
Soil	2	Dried, 105°C, 24 h	^{220}Rn	0.09–0.10[e], 0.12–0.15	50
Sand	1	Saturated	^{222}Rn	0.243	49
Uranium Ore	6	Saturated	^{222}Rn	0.19 ± 0.10 (0.06–0.26)	55
		Dried, 110°C[f]		0.05 ± 0.03 (0.014–0.07)	
Uranium Ore (crushed)	17	Moist, saturated	^{222}Rn	0.28 ± 0.16 (0.055–0.55)	54
		Vacuum-dried		0.14 ± 0.11 (0.023–0.36)	
Tailings	2	Saturated	^{222}Rn	0.29, 0.31	55
		Dried, 110°C[f]		0.067, 0.072	

[a]Arithmetic mean ± one standard deviation (range of values).
[b]Sample sieved through 20 μm mesh.
[c]Sample of six giving highest reading.
[d]Exposed to laboratory air for several days.
[e]This sample, when moist, had an emanation coefficient for ^{220}Rn of 0.13.
[f]Dried to constant weight.

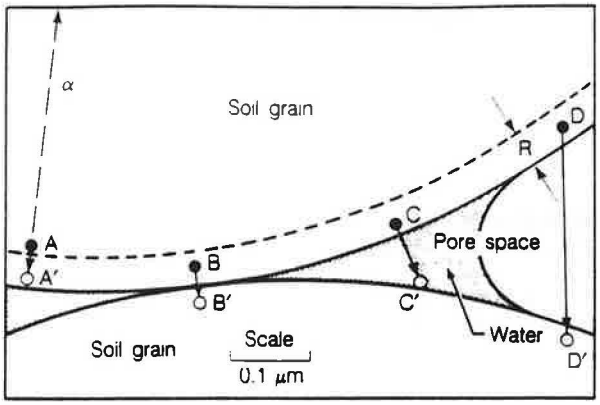

Figure 2.6. Schematic illustration of radon recoil trajectories in and between soil grains. Two spherical grains of 2-μm diameter (clay/silt) are in contact at point B. The stippled portion of the pore is water-filled. The recoil range, R, of the radon atoms is indicated by the dashed line. ^{226}Ra atoms, indicated by solid circles, decay, producing an alpha particle and a ^{222}Rn atom, which may end its recoil at the point indicated by the open circle. At A the radium atom is too deeply embedded within the grain for the radon atom to escape. At B and D the recoiling radon atom possesses sufficient energy after escaping the host grain to penetrate an adjacent grain. At C the radon atom terminates its recoil in the pore water. From Ref. 48, used by permission.

diffusion of radon in intact grains suggests that the diffusion fraction is entirely negligible: diffusion coefficients for argon in rock-forming minerals were measured to be 10^{-31}–10^{-69} m^2 s^{-1} (38); corresponding radon diffusion lengths are 10^{-13}–10^{-32} m.

Two hypotheses have been advanced to account for the large discrepancy between measured and theoretical emanation coefficients (38, 48). The first is that radium is not distributed uniformly but rather is concentrated in secondary crusts or films on the surfaces of the grains. The second hypothesis suggests that chemical corrosion and, particularly, radiation damage due to the decay of its precursors, damages the crystalline structure in the vicinity of the newly formed radon atom, thereby permitting it to migrate more readily than would otherwise be possible. These hypotheses are not mutually exclusive, and both are substantiated by experimental data.

The first hypothesis is supported by the results of two studies. In one, the ^{226}Ra and ^{224}Ra concentrations of two soil samples were measured as a function of grain size and found to decrease nearly monotonically as grain size increased (50). This trend would be expected if a portion of the radium content of each grain were contained in a surface layer. The second study measured ^{238}U and ^{232}Th series concentrations in 70 soil samples and found them to vary linearly with the fraction of the soil mass having particle diameter less than 20 μm (51). Tanner suggests that uranium and thorium are not compatible with the crystalline structure of major minerals and, hence, are commonly found in accessory minerals, adsorbed on the surface of clay particles, or are present in other coatings (48).

Data supporting the second hypothesis come from a study by Barretto of the

effect of annealing rocks, sands, and minerals (52). Invariably, for the six samples studied the radon emanation coefficient dropped as the annealing temperature was increased. For heating to 1000°C, the average (± one standard deviation) of the emanation coefficient of the annealed sample, divided by its original emanation coefficient, was 0.23 (± 0.23).

Additional pertinent evidence is contained in the results of a study of radon emanation from the island of Hawaii (53). The ^{222}Rn emanation coefficient was found to be much smaller for samples from lava fields (average 0.02) than for samples from either thin organic soils (0.55) or deep agricultural soils (0.70). Being of recent origin, and formed by the rapid cooling of a molten solid, lavas would be expected to have relatively uniform distribution of ^{226}Ra and minimal radiation damage. Consequently, their much lower emanation coefficient is not surprising.

Moisture content has been demonstrated in several studies to have a large impact on the emanation coefficient (54–57). Data showing this effect for uranium ore tailings are presented in Figure 2.7. The explanation for this phenomenon appears to lie in the markedly lower recoil range for radon in water than in air. A radon atom entering a pore that is partially filled with water has a very high probability of terminating its recoil in the water. From there, it is readily transferred to the air in the pore. At equilibrium, the partitioning between air and water is described by Henry's law (see Chapter 4). Mass transfer from water to air is rapid: an aqueous diffusion coefficient of order 10^{-9} m^2 s^{-1} (58) and a water layer thick-

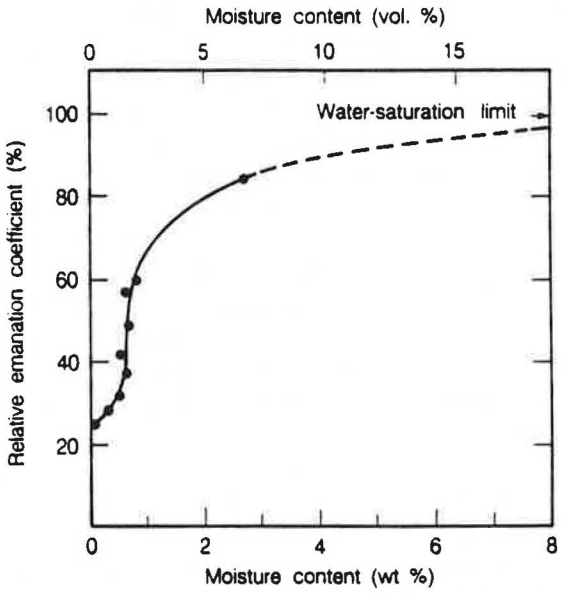

Figure 2.7. Effect of moisture content on ^{222}Rn emanation coefficient for a sample of uranium mill tailings. From Ref. 55. Reproduced from *Health Physics*, Vol. 42, p. 30, by permission of the Health Physics Society.

ness of order 10 μm suggest a characteristic time for transport to the air of 0.1 s; thus equilibrium is achieved rapidly.

The characteristic pore dimension of a soil is related to its grain-size distribution. For a soil having a narrow distribution of grain sizes, the characteristic pore size is the same order as the characteristic grain size. Hence, even for clayey soils, for which the characteristic grain size is of order 1 μm, the pore dimensions are much larger than the radon recoil range in water. Consequently, one would expect the dependence of emanation coefficient on moisture content in most soils to show the general trend indicated in Figure 2.7. As a soil is dried from saturation, the emanation coefficient drops slowly at first as the gravitational water is removed. Once the large pores are drained and capillary water begins to be affected, the emanation coefficient drops substantially. Finally, when only adsorbed water remains, there is little effect of further drying of the soil. This layer is too thin to be very effective in stopping the recoiling radon atoms.

In combination with the discussion in previous sections, this suggests that radon release from soil, combining emanation and transport, is maximal when the soil is moist. Having the small pores filled with water results in a high radon emanation coefficient, but—as most transport takes place through the larger pores—only reduces radon transport to a small degree. When dry, the soil has slightly enhanced transport, but a greatly reduced emanation coefficient. When wet, the emanation coefficient is slightly higher, but the diffusivity and permeability are greatly reduced. This intermediate level of moisture, corresponding approximately to the range between the wilting point and field capacity, is the most common state of natural soils.

To account for the moisture dependence of the emanation coefficient of radon from 17 samples of crushed ore, Thamer et al. proposed the following model (54). The ore was assumed to consist of radioactively inert rock grains held together by a porous cementing material. The pores were treated as cylinders with diameters varying according to a measured pore-size distribution. The radium in the sample was assumed to be uniformly distributed within an annular region of constant thickness around each pore. Finally, moisture was assumed to occur in layers of equal thickness on the inner surface of the radium-bearing annulus.

Two parameters were allowed to vary to fit the data: the inert rock fraction determined the magnitude of the dry emanation coefficient, and the thickness of the radium-bearing annular regions determined the ratio of saturated to dry emanation. With this model, the researchers were successful in matching the dependence of the emanation coefficient on moisture in most cases. Their model yielded values of 0.78 ± 0.11 for the inert rock fraction and 0.025 ± 0.011 μm for the thickness of the radium-bearing regions.

Temperature has also been found to be a factor in determining the radon emanation coefficient, although over the range of temperatures common for surface soils this effect is of minor importance. Stranden et al. (56) found that the radon exhalation rate for a soil sample increased by 55% when the temperature was increased from 5 to 50°C. They suggested that the increase with temperature may be due to a reduction in physical adsorption. Barretto (52) found a much smaller temperature dependence for the emanation coefficient of a granite sample: 0.106

at 265°C to 0.081 at −20°C. He found though that when the sample was cooled to −80°C, the emanation coefficient decreased markedly to 0.028. On the other hand, Tanner (59) found the rate of emanation of radon from a natural, uranium-mineralized, very permeable sandstone core to decrease with increasing temperature over the range of 24–100°C. The results were reversible, indicating that the observed effect was probably not due to changes in moisture content.

Radon condenses at temperatures much lower than those found in the environment. For a pure sample at standard pressure, the boiling point and melting point are −62°C and −71°C, respectively (60). At very low partial pressures, i.e., under all environmental conditions, radon condenses on surfaces at approximately −150°C (61). Common experimental techniques used to concentrate radon from an airstream involve collecting the radon on activated charcoal cooled to the temperature of solid CO_2 (−78.5°C) (62) or on glass wool cooled to the temperature of liquid N_2 (−196°C) (63).

4 BUILDING CHARACTERISTICS

Two aspects of building design and operation play key roles in influencing radon entry from soil. One is the design and operation of the ventilation system, which may affect the pressures that drive bulk airflow through the soil. The second is the design and construction of the building substructure, which controls the degree of movement between the air in the soil and the air in the building.

In addition to these factors, the very presence of a house may influence the spatial distribution of soil moisture and, thereby, the emanation and migration of radon. Except for one anecdotal report (64), such effects have not been documented; however, they seem reasonable to expect based on common experience. For example, a house serves as an umbrella to precipitation such that the soil underlying it tends to be drier than the surrounding uncovered soil. As we have seen, the moisture content of soil is an important factor influencing radon emanation, effective diffusion coefficient, and soil permeability.

A comprehensive treatment of building practices that influence radon entry is beyond the scope of this book. Even within a single country, relevant construction practices vary widely, depending principally on the purpose of the building, the climate, and the structural and drainage characteristics of the local soil. In the United States, construction practices are governed for the most part by municipal codes, rather than by federal or state guidelines. The discussion in this chapter covers only some of the key features of building practice pertaining to radon entry and focuses on single-family residential structures, which have been the most extensively studied. Further discussion may be found in Chapter 10.

4.1 Ventilation

Ventilation refers to the total supply rate of outdoor air into a building, whether intentional or not. It serves the purpose of controlling odors, maintaining a proper balance of metabolic gases, and diluting pollutants generated by indoor sources.

The most important aspect of ventilation for radon entry from soil is its relationship to the pressure difference between the base of the outside walls and the building's substructure openings. This relationship is discussed explicitly in Section 6.2. Here, our objective is to provide a brief introduction to building ventilation. This discussion complements Section 8.2 of Chapter 1.

The ventilation rate has three components. Infiltration refers to the uncontrolled leakage of air into the building through cracks and holes in the building shell. Natural ventilation is the flow of air into the building through open doors and windows. Mechanical ventilation is the provision or removal of air by means of blowers or fans.

In most single-family dwellings in the United States, at times when the outdoor air must be heated or cooled for thermal comfort, infiltration is the predominant component of ventilation. The forces that drive infiltration arise from wind and buoyancy; these are discussed quantitatively in a later section of this chapter. Models have been developed that predict infiltration on the basis of the wind speed (including corrections for local shielding), temperature difference, and leakiness of the structure (see Chapter 1, Section 8.2) (65). Data on infiltration rates in U.S. housing are presented in Chapter 4.

At times when the outdoor air temperature is in the approximate range of 15–25°C, depending on the habits of the building occupants, the rate of natural ventilation may become very large, and the indoor-outdoor pressure differences very small. Concentrations of radon and its progeny inside a residence with open doors and windows are typically close to the outdoor levels.

A major difficulty with the use of infiltration as the principal means of ventilating a building is the lack of control. A building with a relatively large leakage area may be uncomfortably drafty when weather conditions are severe. Rising energy prices beginning in 1973 led to financial pressures to reduce infiltration rates. But during mild weather, the infiltration rate of a "tight" building may be so low that moisture, odor, or other indoor air quality problems result. Consequently, there is considerable interest in the use of mechanical ventilation systems in residential buildings.

A balanced mechanical ventilation system is designed to operate with equal amounts of supply and exhaust air, often passed through a heat-recovery device to reduce energy costs (66). In this case, its effect on the pressure distribution across the base of the building walls is probably negligible. Alternatively, in an unbalanced system, either exhaust or supply ventilation is provided in excess. For example, in a supply-only system, the pressure inside the building is increased, and air flows out either through designed penetrations or through leaks in the building shell. This approach should in principle have the beneficial side effect of reducing radon entry by lowering, or even reversing, the pressure gradient in the surrounding soil. Caution must be exercised to avoid material damage in cold climates owing to the freezing condensation of moisture in exfiltrating air.

Mechanical systems provide the ventilation in most commercial buildings, although small ones may be ventilated like residences. Common commercial design specifies a higher rate of fresh-air supply than exhaust, so that the building is operated at a pressure slightly higher than ambient.

Intermittent activities of the building occupants may influence radon entry by altering the indoor-outdoor pressure differences. Fireplace operation can, because of the large rate of airflow out of the chimney, lower the pressure in a house and significantly increase the air-exchange rate (67). In the only case studied, a concomitant increase in the rate of radon entry was observed that nearly compensated for the increased ventilation rate (2). This result suggests that the use of exhaust fans for local (or general) ventilation may have the undesirable side effect of increasing radon entry rates. Recent modeling of this situation suggests that exhaust ventilation may be a suitable, but not optimal, method of providing air exchange for crawl-space houses and for basement houses surrounded by low-permeability ($< 10^{-12}$ m^2) soil (120). Exhaust ventilation is not recommended for basement houses with highly permeable soil unless measures are taken to impede soil gas entry.

4.2 Substructure

Single-family dwellings in the United States are most commonly built with the lowest floor made either of poured concrete and in direct contact with the underlying soil, or of wood and suspended above the soil. In the former case, the floor may lie below the soil grade; this is designated a basement substructure. Alternatively, the floor may be built to the same level as the soil surface, a substructure type often called "slab-on-grade." The substructure for a house having a suspended wood floor is known as a crawl space.

Each type has unique characteristics that influence radon entry, with the greatest differences occurring between crawl-space substructures and the others. Among the three types, radon entry into basements has received most of the research and remedial attention (1–3, 68–70), but entry into slab-on-grade (71) and crawl-space houses (64) has been studied as well.

The influence of the building substructure on radon entry can be separated into two factors: the degree of coupling between indoor air and soil air, and the size and location of openings and penetrations through the substructure.

Consider first the degree of coupling. The interior of a slab-on-grade or a basement house is potentially well-coupled to the nearby soil. Recommended construction practice calls for the concrete slab to be underlaid by a layer of gravel or crushed stone that, in turn, lies on the subsoil (72). An intermediate plastic membrane may be present, depending on the normal moisture conditions of the surrounding soil. Any penetrations through the concrete and plastic sheeting, if present, constitute a link between the underlying soil and the indoor air that is distributed by means of the gravel layer to the entire area beneath the floor. If the pressure inside the house is reduced with respect to the pressure at the base of the outside walls, that pressure differential is effectively applied across the underlying soil. If the soil is sufficiently permeable, a large radon entry rate can result. Even in the absence of a gravel layer, a basement or slab-on-grade house is closely coupled to the soil.

A house with a crawl-space substructure may be well-coupled to the underlying soil or not, depending on whether the crawl space is vented. The venting generally

required to prevent moisture damage, e.g., 0.67 m^2 of vent area per 100 m^2 of floor area (73), is sufficient in principle to uncouple the indoor air from the soil: essentially all air flowing through the floor of the living space enters the crawl space through the vents, rather than through the soil. Consequently, very high radon entry rates due to elevated soil gas influx, as sometimes found in houses with a basement, are not expected in houses having a vented crawl space.

On the other hand, if the crawl space is unvented and the underlying soil exposed, then the house is well-coupled to the soil, and the radon entry rate may be large. One study conducted in Illinois found that in 9 of 22 such houses indoor radon concentrations exceeded 180 Bq m^{-3} and in six of these the concentration was greater than 370 Bq m^{-3} (74).

Penetrations in the building shell that are most important for radon entry are those through the floor and, in the case of a house with a basement, those through the wall below soil grade. Common routes of entry and means of sealing them are discussed thoroughly in Chapter 10. We note here only a few points in this regard.

Penetrations in the floor of a slab-on-grade or basement house are commonly found at the floor-wall joint, around service entrances (particularly for water supply pipes and the sanitary sewer lines), and in association with floor drains or perimeter drainage systems. The size of these penetrations is almost invariably great enough so that the principal resistance to airflow through the soil and building substructure is in the soil. Hence, for radon entry into concrete-floored houses, the absolute size of penetrations, unless unusually small, is relatively unimportant. The relative size among penetrations and their position may be important. By influencing the length of the path that air must traverse through soil before entering the substructure, these latter factors play a role in determining the volume of soil that may contribute its radon to the indoor air.

In a crawl-space house, penetrations may be found along the foundation sill plate, and around plumbing and sewer pipes, electrical wiring, and heating and air-conditioning ducts where they pass throug the floor. As suggested by the previous discussion, if the crawl space is vented, these penetrations probably have little effect on radon migration through the nearby soil. Their total size does, however, influence radon entry by affecting the proportion of radon entering the crawl space from the soil that enters the house, rather than exiting to the outside air.

5 RADON MIGRATION IN SOIL

In this section, we develop a mathematical formulation describing the radon concentration in the pore air of a differential volume of soil. The equation accounts for the transport of radon by molecular diffusion and forced convection and the production and removal of radon by radioactive decay. In addition to the variables described in earlier sections, application of this equation to the problem of radon entry into buildings requires specifying the pressures at the surface of the soil and inside the building and the building geometry. Analytical solutions to this equation do not exist, except for the simplest geometries. Consequently, a complete treat-

ment requires the use of a numerical model, an undertaking that has only recently been started (7, 75–77, 109, 120, 121). Dimensional analysis permits one to identify circumstances under which one or more of the terms of the governing equation become negligible and, consequently, may be ignored, thereby simplifying the detailed quantitative analysis.

We begin with discussions of the Fick's law and Darcy's law, which, respectively, underlie the description of transport due to molecular diffusion and forced convection. A general differential transport equation is then presented. By the use of scaling arguments, conditions are identified under which the problem of analyzing radon migration in soil near a building may be simplified.

5.1 Diffusive Transport—Fick's Law

To begin, we consider a gas made up of two species, A and B. The molar flux of A relative to stationary coordinates may be expressed (58) as

$$\mathbf{N}_A = x_A(\mathbf{N}_A + \mathbf{N}_B) - cD_o\nabla x_A \tag{8}$$

where $\mathbf{N}_A$ and $\mathbf{N}_B$ are the fluxes of A and B, respectively, with respect to fixed coordinates (moles m^{-2} s^{-1}), x_A is the molar fraction of A in the mixture, c is the molar concentration of the gas (moles m^{-3}), D_o is the diffusion coefficient (m^2 s^{-1}) (see Section 2.3), and ∇ is the three-dimensional gradient operator. The first term on the right-hand side of Equation 8 represents the flux density of A due to convection, and the second term gives the diffusional flux density relative to the mean convective velocity. This expression embodies Fick's first law, which states that the diffusional flux density is proportional to the concentration gradient. Fick's law is based on experimental observations and is consistent with the postulates of kinetic theory for an ideal gas. Other physical conditions that may lead to a diffusive flux, in particular temperature gradients, pressure gradients, and external forces (e.g., due to an imposed electric field), are neglected in this expression. They are usually unimportant relative to the concentration gradient.

For the case of radon in air, we can make major simplifications in Equation 8. First, since the mole fraction of radon in air is always vanishingly small (40,000 Bq m^{-3}, a typical concentration in soil air, is equivalent to a mole fraction of ^{222}Rn of 7.6×10^{-16} at 20°C), the molecular diffusion of radon may be neglected as a source of convection of the mixture. That is, we may neglect the term $x_A\mathbf{N}_A$ as small compared to $\mathbf{N}_A$. A further simplification results from approximating the molar concentration of air as a constant. Hence,

$$\mathbf{N}_{Rn} = x_{Rn}\mathbf{N} - D_o\nabla c_{Rn} \tag{9}$$

where $\mathbf{N}$ is now the molar flux density of air relative to stationary coordinates and $c_{Rn} = cx_{Rn}$ is the molar concentration of radon. It is convenient to multiply this equation by Avogadro's number and the decay constant of radon so that

$$\mathbf{J}_{Rn} = I_{Rn}\mathbf{V} - D_o \nabla I_{Rn} \tag{10}$$

where I_{Rn} is the activity concentration of radon (Bq m^{-3}), $\mathbf{J}_{Rn}$ is the activity flux density (Bq m^{-2} s^{-1}), and $\mathbf{V} = \mathbf{N}/c$ is the net air velocity (m s^{-1}). The discussion in this section focuses on the implications of the diffusive flux ($-D_o \nabla I_{Rn}$). The convective flux ($I_{Rn}\mathbf{V}$) is discussed in the following section.

Before proceeding, it is worthwhile to note a potentially important assumption implicit in Equations 8–10. We have treated radon in air as an effectively binary mixture. This means that we neglect any transport of radon that may result from the diffusion of another species in air (except as that diffusion causes convection of the mixture). Whether multicomponent diffusion effects are important for radon migration in soil is not known. A case that may prove to be significant is radon migration due to the diffusion of water vapor. Further discussion of multicomponent diffusion may be found in Ref. 58.

Thus far in this section, we have assumed the radon to be migrating in open air. Considering the diffusion of radon in soil, we need to adjust our description to account for two effects of the solid matrix: the area through which radon may diffuse is reduced and the average path length that radon must traverse to reach one point from another is increased. These factors are embodied in the replacement of the binary diffusion coefficient, D_o, with an effective diffusion coefficient, D_e, so that

$$\mathbf{J}^d_{Rn} = -D_e \nabla I_{Rn} \tag{11}$$

In this equation, $\mathbf{J}^d_{Rn}$ represents the diffusive flux density of radon activity per unit of pore area of the soil. The relationships among D_e, D (the bulk diffusion coefficient), and D_o were discussed in Section 2.3.

Two implicit approximations remain in the description of diffusive flux given in Equation 11. It is worthwhile to examine them briefly before continuing. First, we have assumed that, as in open air, all the kinetic interactions of the radon atoms occur with gas molecules. This is a reasonable approximation so long as the pores are large relative to the mean free path of the radon atoms, which is comparable with that for the major constituents of air, 0.065 μm at 25°C. Pore dimensions are of the same order as grain size; hence, for all soils larger than clays, this assumption is good. For smaller pores, the molecular transport process is termed Knudsen diffusion. The flux density remains proportional to the concentration gradient; however, the diffusivity is proportional to the pore radius and thus is a strong function of position within the pores (78).

The second approximation is that all radon in the soil exists in one of two states: within the air contained in the soil or within the solid soil grains. This approximation embodies at least three simplifications. First, we are treating the pore size distribution as unimodal, or, in the parlance of Currie (39), we are treating the soil as solid grained, rather than crumbly. Alternatively, we are assuming that the characteristic time for transport out of the small pores of a grain into the major pores of the soil matrix is small relative to the transport time through the major pore.

The second simplification neglects the fraction of radon that is present in soil water. At 20°C, the coefficient of solubility, defined as the ratio of concentrations at equilibrium, for radon between water and air is 0.25 (79). If the moisture saturation is 50% and the temperature is 20°C, the amount of radon in the gas phase of the pores is 4 times as large as that in the water phase. This effect will be considered explicitly below. Finally, we neglect any possible adsorption of radon on the surfaces of the soil grains. As radon is an inert gas, and its condensation temperature is much lower than environmental temperatures, this would seem to be a good assumption. Experimental evidence of the effect of adsorption on radon release from geological materials has been reviewed by Tanner (48). He concluded that the studies were insufficient to determine whether this is an important factor.

For a dry, solid-grained soil through which radon migrates only by diffusion, the activity concentration in the pores is described by the following conservation-of-mass equation:

$$\frac{\partial I_{Rn}}{\partial t} = D_e \nabla^2 I_{Rn} - \lambda_{Rn} I_{Rn} + G \tag{12}$$

where λ_{Rn} is the decay constant of radon (2.1×10^{-6} s^{-1} for ^{222}Rn and 0.0125 s^{-1} for ^{220}Rn), and G is the volumetric radon generation rate in the soil pores (Bq m^{-3} s^{-1}). We have assumed that the diffusion coefficient is constant. The generation rate may be determined from parameters already introduced:

$$G = f\rho_s A_{Ra} \lambda_{Rn} \frac{1 - \epsilon}{\epsilon} \tag{13}$$

where f is the emanation fraction, ρ_s is the density of the soil grains [commonly 2.65×10^3 kg m^{-3} and rarely not in the range $(2.6\text{–}2.8) \times 10^3$ (9)], A_{Ra} is the radium activity concentration in the soil (Bq kg^{-1}), and ϵ is the porosity.

Considering the case of uncovered soil of infinite depth and extent, and assuming the radon concentration to be zero at the soil surface, the steady-state solution to the one-dimensional form of Equation 12 yields the radon activity concentration in the soil pores at a depth z below the surface:

$$I_{Rn}(z) = I_\infty (1 - e^{-z/l}) \tag{14}$$

where $I_\infty = G/\lambda_{Rn}$ is the activity concentration of radon in the pores at large depths and $l = (D_e/\lambda_{Rn})^{1/2}$ is known as the diffusion length. For ^{222}Rn, a typical value of l is 1 meter or less.

The flux density of radon from uncovered soil due entirely to diffusion is given by multiplying Equation 11 by ϵ so that the flux is determined per unit geometric area. Substituting Equation 14, we obtain the result

$$J_{Rn}^d = \epsilon \lambda_{Rn} l I_\infty = (D_e \lambda_{Rn})^{1/2} \rho_s f A_{Ra} (1 - \epsilon) \tag{15}$$

Taking as typical values for ^{222}Rn, $D_e = 2 \times 10^{-6}$ m^2 s^{-1}, $\rho_s = 2.65 \times 10^3$ kg m^{-3}, $f = 0.2$, $A_{Ra} = 30$ Bq kg^{-1}, and $\epsilon = 0.5$, we obtain $J^d_{Rn} = 0.016$ Bq m^{-2} s^{-1}. By comparison, Wilkening et al. (28) estimated the mean worldwide flux of ^{222}Rn to be approximately 0.015 Bq m^{-2} s^{-1}.

Because of its much larger decay constant, the activity flux of ^{220}Rn should generally be larger than that of ^{222}Rn, although the molar flux should be substantially less (see Chapter 1, Section 8.4). Flux of ^{220}Rn from dry, uncovered soil measured at six sites in New Mexico was found to be 1.6 ± 0.3 Bq m^{-2} s^{-1} (80), 100 times larger than the typical value for ^{222}Rn cited above, but, in molar terms, 60 times less.

The diffusion of radon from soil through concrete slabs and into houses has been analyzed theoretically (81–84). The results show that a structurally intact slab is an effective barrier against radon entry: a reduction in flux to approximately 5% or less of the value for uncovered soil is expected for a typical case (82, 85). Experimental measurements of flux through concrete slabs confirm that the diffusion of radon through concrete is much less than needed to account for radon in houses (1). If the slab is cracked, the diffusional flux may be greatly increased. Landman (83) determined that 25% of the flux from uncovered soil would penetrate the slab if a 1-cm gap existed for every 1 m of slab. Even for relatively large penetrations, however, the resulting diffusive flux is still much smaller than the observed entry rates in most houses.

In addition to affecting the emanating fraction and the diffusion coefficient, the presence of water in the soil pores alters the diffusive transport equation. If we assume that radon is partitioned between water and air according to Henry's law, and that diffusion of radon within the water can be neglected, then the transport equation can be written

$$\frac{1}{\epsilon}\frac{\partial(I_a\epsilon_a + I_w\epsilon_w)}{\partial t} = D'_e\nabla^2 I_a - \frac{1}{\epsilon}\lambda_{Rn}(I_a\epsilon_a + I_w\epsilon_w) + G' \qquad (16)$$

where I_a is the radon concentration in the air volume, I_w is the radon concentration in the water volume, and ϵ_a and ϵ_w are the air and water porosities, respectively, so that $\epsilon_a + \epsilon_w = \epsilon$. The radon concentrations in the two phases are related by $I_w = \kappa I_a$, where κ is the coefficient of solubility of radon in water. The solution to the steady-state problem for a semiinfinite soil is analogous to Equations 14 and 15 with modified diffusion length, infinite depth concentration, and surface flux.

$$l = \left[\frac{\epsilon}{\epsilon_a + \kappa\epsilon_w}\right]^{1/2}\left[\frac{D'_e}{\lambda_{Rn}}\right]^{1/2}$$

$$I_\infty = \frac{G'\epsilon}{\lambda_{Rn}(\epsilon_a + \kappa\epsilon_w)}$$

$$J^d_{Rn} = (D'_e\lambda_{Rn})^{1/2}\rho_s f' A_{Ra}(1 - \epsilon)\left[\frac{\epsilon_a}{(\epsilon_a + \kappa\epsilon_w)\epsilon}\right]^{1/2} \qquad (17)$$

For $\epsilon_a = \epsilon_w = 0.25$ and $\kappa = 0.25$, and assuming that moisture has no effect on D_e and f, l is increased by 26%, I_∞ is increased by 60%, and J^a_{Rn} is decreased by 37%. Of course, in general, the change in moisture has a substantial effect on both D_e and f. For example, the results presented in Figures 2.4 and 2.7 indicate that for the respective samples, the effective diffusion coefficient is decreased by a factor of 5, and the emanation coefficient is increased by a factor of 4, for the wet case relative to the dry case.

5.2 Convective Transport—Darcy's Law

In the middle of the nineteenth century, H. Darcy conducted experiments on the flow of water through sand columns. His results showed that for a given column the volumetric flow rate, Q, was proportional to the difference of the fluid heads at the inlet and outlet of the column, Δh, and to its cross-sectional area, A, and inversely proportional to the length of the column, L:

$$Q = \frac{c_1 \Delta h A}{L} \tag{18}$$

where c_1 is a constant dependent on the sand. Muskat (13) argued theoretically that the relationship

$$v = \frac{Q}{A} = \frac{c_2 d^2}{\mu} \frac{\Delta p}{\Delta L} \tag{19}$$

should hold under restricted conditions. In this expression, c_2 is a constant, d is a length scale related to the soil grain size or pore diameter, μ is the viscosity of the fluid, and $\Delta p / \Delta L$ represents the pressure drop per column length. The derivation of this equation follows from dimensional analysis and the postulate that, for sufficiently low Reynolds numbers ($\mathrm{Re} = dv_i\rho/\mu$, where v_i is the interstitial fluid velocity and ρ is the fluid density), the flow through a porous material should be analogous to viscous flow through a pipe, as described by Poiseuille's law (58). In deriving Equation 19 and throughout the discussion that follows, the effects of gravity are neglected.

Equation 19 can be converted to differential form by allowing ΔL to become infinitesimal. Then, if the soil permeability is constant and isotropic, Darcy's law may be written

$$\mathbf{v} = -\frac{k}{\mu} \nabla P \tag{20}$$

where $\mathbf{v}$ is the superficial velocity vector, i.e., the flow per unit geometrical area defined over a region large relative to individual pores but small relative to the overall dimensions of the soil; k is the intrinsic permeability as discussed in Section

2.2; and ∇P is the pressure gradient. This expression appears to be valid even if the permeability is not constant.

If the soil permeability is not isotropic, the permeability coefficient is replaced with a 3×3 permeability matrix, $\mathbf{K}$, and Darcy's law becomes (9, 12, 24)

$$\mathbf{v} = -\frac{1}{\mu}\mathbf{K} \cdot \nabla P \tag{21}$$

Given the superficial air velocity through soil, the radon activity flux per unit pore area due to convective flow is expressed by

$$\mathbf{J}_{Rn}^{c} = \frac{I_{Rn}\mathbf{v}}{\epsilon} \tag{22}$$

Darcy's law has been observed to break down as the Reynolds number increases. In contrast to viscous flow in pipes, for which Poiseuille's law remains valid for $Re < 2000$, experimental evidence has shown deviations from Darcy's law for Reynolds numbers in the range of 0.1–75 (12). In the case of pipe flow, the deviations are associated with the onset of turbulence. Deviations from Darcy's law with increasing Reynolds numbers are sometimes attributed to turbulence (86). It is more likely, however, that the flow remains laminar and that this effect is due to the emerging importance of the inertial term in the Navier-Stokes equation as the Reynolds number increases through order 1 (12, 58, 87, 88).

Under most circumstances, for the problem of radon entry into buildings, Darcy's law would be expected to hold in the soil. For a typical pressure gradient of 5 Pa m^{-1}, the Reynolds number is less than one for all soils having a permeability less than approximately 10^{-9} m^2, i.e., for all soils finer than gravel.

A second assumption in the development of Darcy's law is, as in the case of applying Fick's law to porous media, that the pores are large relative to the mean free path of the gas. Corrections are possible if this assumption is not true (12); however, determining the fluid velocity analytically becomes more difficult. It seems probable that this refinement is not of great importance in the problem at hand as the pores of soils through which convective flow is likely to be important are generally large relative to the mean free path.

If we assume that Darcy's law holds, we may combine Equation 20 or 21 with a continuity equation and an equation of state to obtain a governing equation for the pressure in the soil. By solving the governing equation for a specified geometry subject to appropriate boundary conditions on the pressure and/or the velocity, we may determine the convective velocity field in the soil, or , alternatively, the volume flow rate, e.g., into a building substructure. The velocity field is needed as input to analysis of the full transport equation, as discussed in the next section. The volume flow rate into the building, combined with an estimate of the radon concentration in the entering air, can be used to compute the radon entry rate attributable to convective flow.

For the remainder of the discussion in this section, we assume Darcy's law accurately describes airflow through soil, and that the soil is homogeneous and isotropic with respect to the permeability. It can be shown that, under these constraints, and for the problem of radon migration in soil, air in the soil may be treated as incompressible and, in steady state, the pressure satisfies the Laplace equation:

$$\nabla^2 P = 0 \tag{23}$$

This is a classic equation in applied physics which arises in connection with problems other than fluid flow in porous media, including electrical potential in the vicinity of charged bodies (89), fluid flow at high Reynolds number outside the boundary layer (87), and heat conduction in solids (90). Consequently, there is a considerable literature on methods of solving Laplace's equation. Analytical solution methods include conformal mapping and separation of variables through a coordinate transformation (91). The latter approach can be valuable for radon entry if the building being investigated has, or can be approximated as having, certain symmetry (2, 92). A graphical technique called flow-net sketching is useful if the problem can be treated as two-dimensional and the pressure at the surface of the soil is assumed to be constant (9, 10). It yields the fluid streamlines and isopotential lines and can be used to estimate the velocity field and the total flow rate. Similar results with similar constraints can be obtained from an experimental technique using the electrical analog to the fluid flow problem (9). The most powerful and flexible technique is numerical modeling using a finite-element method (93). It is also the most costly to develop and implement.

Several workers have reported on investigations of aspects of convective radon migration in soil for applications other than radon entry into buildings (49, 94–100). Of particular interest are the results of the studies in New Mexico of radon exhalation from uncovered soil. Clements and Wilkening (98) found that barometric pressure changes of 1000–2000 Pa over a period of 1–2 days produced convective velocities of order 10^{-6} m s^{-1} at the surface of a soil with permeability of 10^{-12} m^2. The radon flux from the surface was thereby changed by 20–60% compared to the rate associated with molecular diffusion alone. We shall see that this is a small effect for a large change in pressure relative to the effects of pressure differences on radon entry into buildings.

In a later study in gravelly sandy loam in the same area, Schery et al. (100) concluded that among the possible environmental influences leading to temporal variation in radon exhalation, atmospheric pressure changes and rainfall were the most important. Effects due to temperature and wind were either comparatively small or undetectable. The time-averaged radon flux from the uncovered soil surface was close to that expected for pure molecular diffusion. Based on an observed inconsistency between the near-surface radon concentration profile and the measured flux density, the investigators suggested that a contribution to the exhalation rate may have resulted from direct flow through inhomogeneities.

These studies suggest that molecular diffusion dominates convection as a process by which radon enters the atmosphere from uncovered soil. As is discussed in more detail in subsequent sections, the reverse is often true for buildings. There are two major differences between these cases. First, a building's substructure shell is an effective barrier to molecular diffusion, thereby reducing its importance. Second, the geometry of a building and its operation lead to sustained pressure differences which may induce small, yet persistent, airflows into a building through the soil. Such sustained flows generally do not exist for horizontal surfaces of uncovered soil.

5.3 General Transport Equation

Following the discussion of the previous two sections, we may combine the effects of diffusion and convection into a general transport equation for radon migration in soil. For soil with negligible moisture content, the result is

$$\frac{\partial I_{Rn}}{\partial t} = \nabla \cdot D_e \nabla I_{Rn} - \nabla \cdot I_{Rn} \frac{\mathbf{v}}{\epsilon} + f\rho_s \frac{1-\epsilon}{\epsilon} A_{Ra}\lambda_{Rn} - \lambda_{Rn} I_{Rn} \qquad (24)$$

If the moisture content of the soil is large enough for a significant fraction of the radon in the pores to be dissolved in the liquid, the transport equation is written

$$\frac{1}{\epsilon}\frac{\partial(I_a\epsilon_a + I_w\epsilon_w)}{\partial t} = \nabla \cdot D_e' \nabla I_a - \nabla \cdot I_a \frac{\mathbf{v}'}{\epsilon_a} + f'\rho_s \frac{1-\epsilon}{\epsilon} A_{Ra}\lambda_{Rn} - \frac{1}{\epsilon}\lambda_{Rn}(I_a\epsilon_a + I_w\epsilon_w) \qquad (25)$$

where the primes indicate new values accounting for the moisture content and where we have neglected any moisture migration and any migration of radon within the water.

As previously noted, these equations have not been solved analytically, except for the simplest geometry (98, 100). Consequently, to make much progress, we are left with two approaches: approximate analysis and numerical modeling. In the remainder of this subsection, we discuss aspects of approximate analysis. In Section 6.3, recent research on modeling radon entry into buildings, a task that is still in its early stages of development, is briefly discussed.

The most significant simplification possible in this problem is to be able to neglect one of the transport processes—molecular diffusion or convection—as negligible compared with the other. To compare the relative importance of the two processes, we make some simplifying assumptions to Equation 24, then make the equation dimensionless. The simplifying assumptions are that (i) the superficial velocity is described by Darcy's law; (ii) the soil is isotropic and homogeneous with respect to the diffusion coefficient, permeability, porosity, emanating frac-

tion, radium content, and bulk density; and (iii) for the range of pressures of interest, air may be treated as incompressible. Then we may write

$$\frac{\partial I_{Rn}}{\partial t} = D_e \nabla^2 I_{Rn} + \frac{k}{\epsilon\mu} \nabla P \cdot \nabla I_{Rn} + G - \lambda_{Rn} I_{Rn} \tag{26}$$

where G is defined by Equation 13.

To make the equation dimensionless (see, e.g., Ref. 58), we multiply and divide each variable by a unqiue combination of a characteristic time λ_{Rn}^{-1}, length L, and pressure difference ΔP_o, as needed to make each dimensionless. Having done so, we may write Equation 26 as

$$\frac{1}{N_\tau} \frac{\partial I_{Rn}^*}{\partial t^*} = \frac{1}{Pe_p} \nabla^{*2} I_{Rn}^* + \nabla^* P^* \cdot \nabla^* I_{Rn}^* + \frac{1}{N_\tau} (G^* - I^*) \tag{27}$$

where the asterisks denote dimensionless quantities. This equation has two dimensionless groups

$$Pe_p = k\epsilon\Delta P_o (\mu D_e)^{-1} \tag{27a}$$

and

$$N_\tau = \Delta P_o k (\mu\epsilon L^2 \lambda_{Rn})^{-1} \tag{27b}$$

The dimensionless groups are important variables: Pe_p, effectively a Péclet number for mass transfer in a porous medium, characterizes the relative importance of convective transport with respect to diffusive transport, and N_τ characterizes the relative importance of radioactive decay with respect to convective flow as a means of removing radon from the soil pores.

Based on the values of these groups, we may simplify the problem as follows. First, if $Pe_p >> 1$, diffusion may be neglected compared with convective flow as a transport process, and the governing equation in dimensional form becomes

$$\frac{\partial I_{Rn}}{\partial t} = \frac{k}{\epsilon\mu} \nabla P \cdot \nabla I_{Rn} + G - \lambda_{Rn} I_{Rn} \tag{28}$$

If $Pe_p >> 1$ and $N_\tau >> 1$, the problem may be treated in steady state and radioactive decay neglected. The resulting equation is analogous to the convective heat transfer problem with internal sources in which conduction and viscous dissipation may be neglected (90).

If $Pe_p << 1$, convective transport may be neglected. The concentration is governed by the diffusion equation (Equation 12). Finally, if $Pe_p << 1$ and $N_\tau >> Pe_p$, the problem reduces to Poisson's equation:

$$\nabla^2 I_{Rn} + \frac{G}{D_e} = 0 \tag{29}$$

Soil permeability is the most important parameter in determining which, if any, of these conditions is satisfied. Choosing typical values of $\Delta P_o = 3$ Pa, $\epsilon = 0.5$, $\mu = 17 \times 10^{-6}$ kg m^{-1} s^{-1}, and $D_e = 2 \times 10^{-6}$ m^2 s^{-1}, then $Pe_p = 1$ if $k = 2.3 \times 10^{-11}$ m^2. Assuming these typical values apply, then for soils with much larger permeabilities, i.e., coarse sands and gravels, transport by molecular diffusion can be neglected. For soils with much smaller permeabilities, i.e., silts and clays not having significant structural permeability, convective transport can be neglected. If we further take $L = 3$ m as the scale of soil length through which transport must be considered, then the permeability at which $N_\tau = 1$ is 5×10^{-11} m^2.

6 RADON ENTRY INTO BUILDINGS

6.1 Pressure-Generating Mechanisms

6.1.1 Wind. Consider the wind blowing directly on the side of a house. In the simplest model, if we neglect the shear stress between the wind and the ground, the change in momentum from the free-stream velocity must equal the increase in pressure at the wall where the velocity falls to zero. Hence

$$\Delta P_o = \tfrac{1}{2} \rho v^2 \tag{30}$$

where ρ is the air density, v is the velocity, and ΔP_o is the pressure at the wall minus the free-stream pressure. This equation may readily be derived from the one-dimensional, steady-state form of the Navier-Stokes equation, i.e., from a momentum balance, assuming the Reynolds number is much greater than one, a condition that for the case at hand is always satisfied.

Actual wind-induced pressures across the walls of a house are moderated from this simple calculation by several factors. Winds generally strike a house obliquely, reducing pressures. The height of a typical house is small enough that the effect of the ground on reducing wind speed is significant. Furthermore, houses are often shielded by other structures and vegetation. In accounting for these effects, wind engineers write Equation 30 as

$$\Delta P = C_d \left(\tfrac{1}{2} \rho v^2\right) \tag{31}$$

where C_d is called the drag or pressure coefficient. It is determined empirically, often from wind tunnel studies. It is found to be relatively independent of wind speed, but greatly dependent on small details of shape, orientation, and shielding (101). In one study, ground-level data for an impermeable cube in a boundary-

layer velocity profile indicated an average drag coefficient of 0.56 on the windward side, −0.49 on the side walls, and −0.15 on the leeward side (102).

These data apply only at the base of the walls, whereas for the problem of radon entry, we are interested in the pressures at the ground surface at distances up to several meters from the walls. A wind tunnel investigation of this matter was recently conducted (77). The results, reproduced in Figure 2.8, show drag coefficients on the windward side of 0.2–0.5 extending distances comparable to the house dimensions.

Taking 0.4 and 3 m s^{-1} as representative values of the windward drag coefficient and wind speed, respectively, and assuming the pressure inside the house is the same as the free-stream conditions, we obtain a pressure difference across the soil and substructure on the windward side of approximately 2 Pa. Note that the pressure difference varies as the square of the wind speed, so that considerably larger pressure differences are possible.

Pressures induced by winds can fluctuate rapidly; so it is important to consider how rapidly pressure fluctuations at the surface of the soil are transmitted through it. This question has been addressed theoretically by Fukuda (103), who obtained

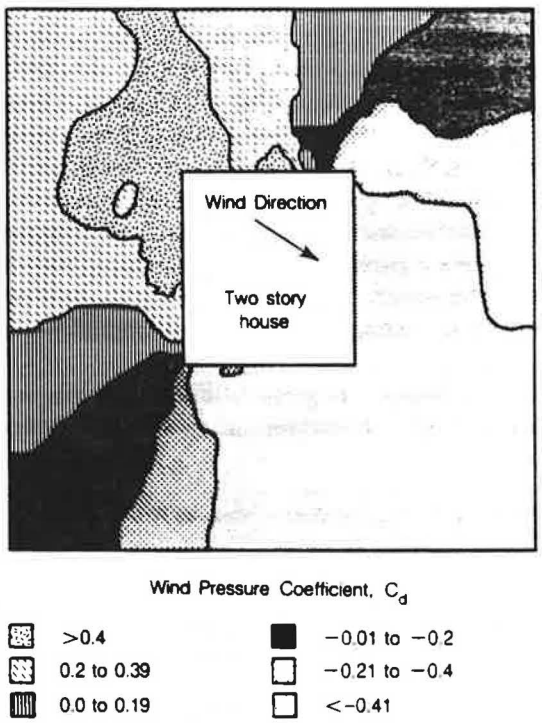

Figure 2.8. Wind pressure coefficient, C_d, at ground surface in vicinity of a model two-story house. Measurements were conducted in a wind tunnel. From Ref. 77. Illustration after A. G. Scott, used by permission.

the following governing equation for the pressure fluctuations, φ, assuming them to be much smaller than the atmospheric pressure, P_a:

$$\frac{\partial \varphi}{\partial t} = \frac{k}{\epsilon \mu} P_a \nabla^2 \varphi \tag{32}$$

where the symbols are as previously defined. This is the diffusion equation; the term $D_p = kP_a(\mu\epsilon)^{-1}$ is a "diffusion coefficient" for pressure disturbances. If, for simplicity, we consider a one-dimensional case, then the characteristic time for a pressure disturbance to propagate through a distance L_p is given by

$$\tau_p = \frac{L_p^2}{D_p} \tag{33}$$

Values of τ_p for L_p = 1 m and 5 m for different soil types are given in Table 2.7. For sandy and gravelly soils, propagation times are minutes or less, whereas for clayey soils, pressure disturbances can take many days to propagate.

Van der Hoven analyzed the spectral distribution of the wind speed at 100 m at Brookhaven, New York (104). As shown in Figure 2.9, reproduced from his results, the wind energy distribution is roughly bimodal, with the low-frequency mode having a peak corresponding to a period of 4 days and the high-frequency mode having a peak at a frequency of about 1 minute. A large spectral gap for periods from about 10 minutes to 2 hours is believed to be generally present. From these data we can conclude that for soils with sufficiently high permeabilities for pressure-driven flow to be important, a large fraction of the wind power is sufficiently sustained so that the pressure disturbance is completely propagated through the soil and a steady-state pressure distribution may be assumed. However, a significant portion of the wind energy occurs with fluctuations at sufficiently high frequency so that the steady-state pressure assumption is not strictly valid.

6.1.2 Temperature Differences. A pressure differential that varies with height exists across any vertical wall separating air masses of different tempera-

TABLE 2.7 Characteristic Times for Propagation of Pressure Disturbances in Soil[a]

Soil type	Permeability (m^2)	τ_p (L_p = 1 m)	τ_p (L_p = 5 m)
Clay	10^{-16}	10 d	250 d
Sandy clay	5×10^{-15}	5 h	5 d
Silt	5×10^{-14}	30 min	12 h
Sandy silt and gravel	5×10^{-13}	3 min	75 min
Fine sand	5×10^{-12}	18 s	450 s
Medium sand	10^{-10}	0.9 s	23 s
Gravel	10^{-8}	0.01 s	0.2 s

[a] $\tau_p = (L_p^2 \mu\epsilon)(P_a k)^{-1}$; $\mu = 17.5 \times 10^{-6}$ kg m^{-1} s^{-1}, $\epsilon = 0.6$, $P_a = 1.01 \times 10^5$ Pa.

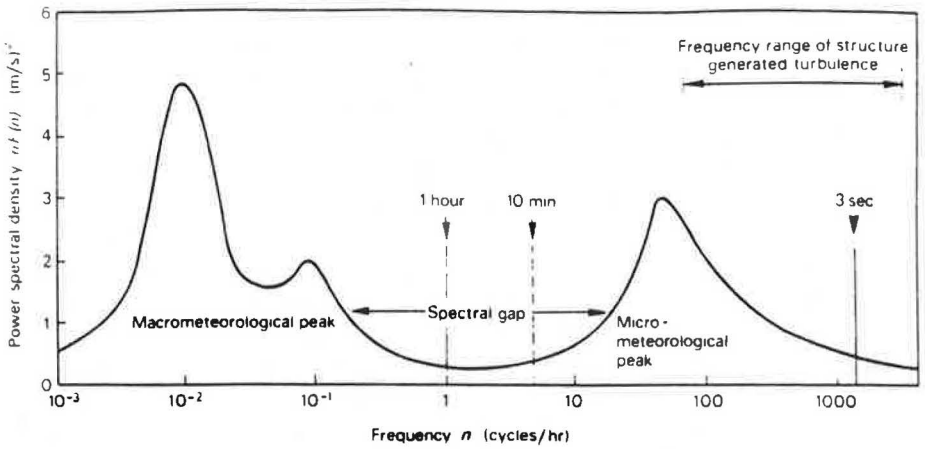

Figure 2.9. Horizontal wind-speed frequency spectrum measured at approximately 100 m height at Brookhaven, NY. From I. Van der Hoven (1957), *Journal of Meteorology*, 14, 160. By permission of the American Meteorological Society.

tures. Otherwise known as the "stack effect," this pressure difference arises because air is a compressible fluid, whose density varies with temperature, and which is acted upon by gravity.

Consider a wall of height H separating air masses of temperature T_i and T_o. If we assume that the ideal gas law applies and that the temperature on either side of the wall is constant, then the conditions of fluid statics require that the pressure vary with height on either side of the wall according to

$$P = P_o e^{-mgz/RT} \tag{34}$$

where P_o is the pressure at reference height $z = 0$; m is the molar weight of air (0.029 kg mol^{-1}); g is the acceleration of gravity (9.8 m s^{-2}); R is the universal gas constant (8.31 J mol^{-1} K^{-1}); and T is temperature. If we now define z_o as the height at which the pressures on either side of the wall are equal, then we find that the pressure difference across the walls is

$$\Delta P(z) \approx \alpha \left[\frac{1}{T_i} - \frac{1}{T_o}\right](z - z_o) \tag{35}$$

where $\alpha = 3454$ Pa m^{-1} K. In deriving Equation 35 we have made the approximation $e^{-x} \approx 1 - x$, valid for $x \ll 1$. As with wind-induced pressure differences, a positive ΔP implies a net inward pressure.

A representative situation has $T_i = 293$ K, $T_o = 273$ K, and $z_o = 3$ m, so that $\Delta P(0) = 2.6$ Pa. Since $|T_o - T_i| \ll T_o$ or T_i for any situation involving an occupied building, the pressure difference due to the stack effect is approximately proportional to the temperature difference.

6.1.3 Other Processes. Several other processes can, in principle, lead to convective flow of soil air into or through building substructures. Here we shall consider two factors: barometric pressure changes and precipitation. These processes are complex, and relatively little work pertaining to them has been reported. Consequently, our discussion will be brief and qualitative.

Compared with the pressure changes associated with winds and temperature differences, the magnitude of barometric pressure changes is large, with excursions from the long-term average routinely exceeding 100 Pa. However, these pressure changes can be effective in inducing the flow of soil air into a building only if they lead to a sustained difference in pressure between the indoor air and the pore air of the nearby soil. An inverse correlation between indoor radon concentration and the rate of change of barometric pressure was observed in the basement of a house in Princeton, New Jersey, during the late spring (69). The authors inferred that the short-term variation in radon entry rate exceeded an order of magnitude for rates of change in pressure from -76 to 45 Pa h^{-1} (-0.75 to 0.44 mbar h^{-1}). In another study, no correlation between radon entry rate into a house with a basement and rate of barometric pressure change was apparent (2).

Although there has been no experimental verification, one might expect to find the influence of barometric pressure changes to be substantial for a house with a basement in relatively permeable soil at a time when the surface of the soil was frozen. Under such circumstances, barometric pressure changes could lead to a flow of soil gas that is "funneled" through the basement as a result of the reduced permeability at the surface of the surrounding soil. A similar situation might exist for buildings with any type of substructure immediately following a heavy rain. Still another case where radon entry rate may be strongly correlated with barometric pressure changes is one in which landscaping has resulted in a low permeability cap over a relatively highly permeable soil.

One expects that the effect of barometric pressure changes on radon entry rate would also depend on the depth of the soil to an impermeable zone. If the air reservoir in the soil were restricted to a small depth below the foundation and above a low permeability layer (e.g., clay or water table), barometric pressure changes should be relatively ineffective in inducing flow.

Through a pistonlike displacement of soil air, a heavy rainfall could potentially lead to a short-term increase in radon entry rate independent of the barometric pressure. At such a time, the permeability of the wet soil surrounding the house is considerably smaller than that of the dry soil beneath it; hence, radon-bearing soil gas could be forced through penetrations in the substructure. Evidence that such an effect might occur is shown in Figure 2.10. During the two-day period of March 29–30, 1983, coincident with a heavy rainfall, radon concentrations indoors and in the crawl space rose to their highest values for the entire 5-week monitoring period. The investigators could not rule out the possibility that the increased concentrations were due to a reduction in permeability of the surrounding soil combined with the concurrent drop in barometric pressure (64).

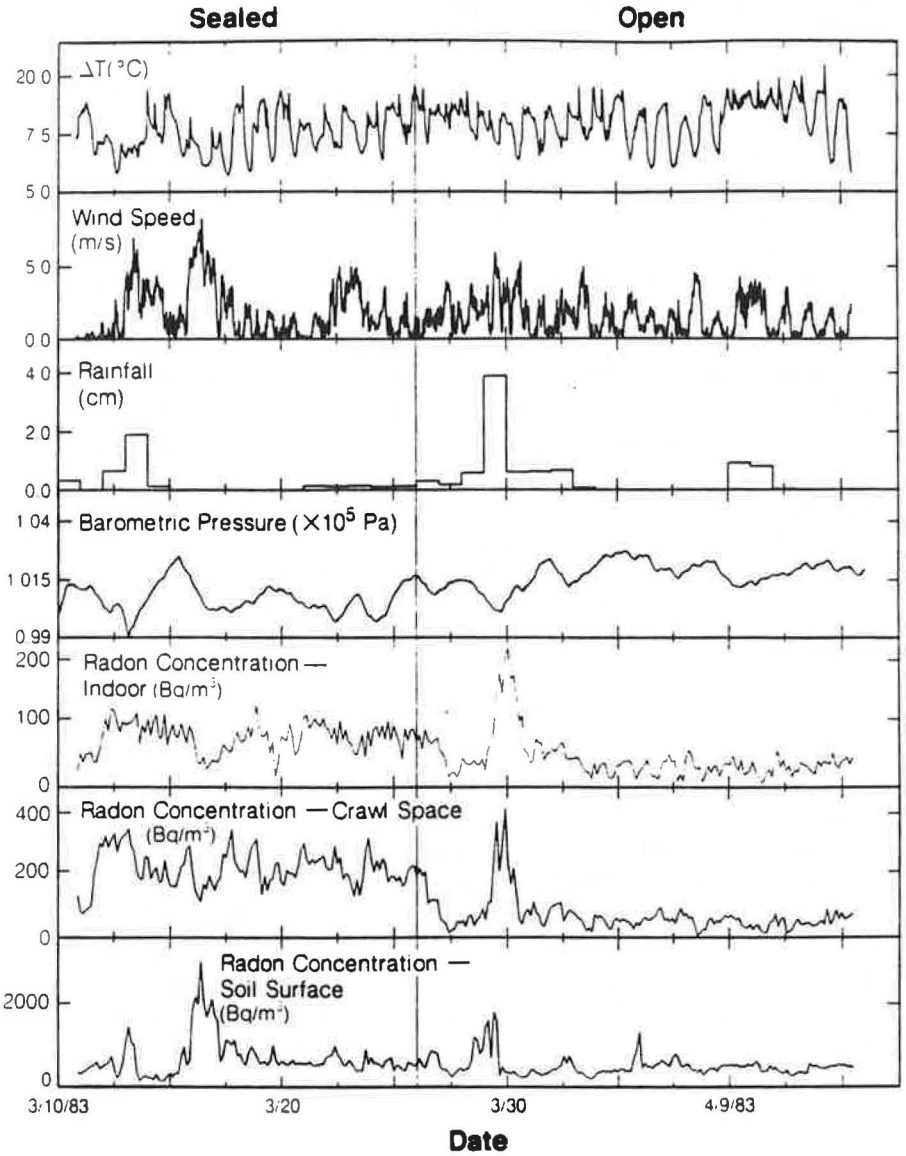

Figure 2.10. ^{222}Rn and meteorological measurements made over a 5-week period at a house with a crawl space in Portland, Oregon. The crawl-space vents were sealed during the first two weeks and open during the final 3 weeks. An episode of enhanced radon flux into the crawl space and house on March 29–30 corresponds to a period of heavy rainfall coupled with a modest drop in barometric pressure. ΔT represents the indoor-outdoor temperature difference. Reproduced from Ref. 64.

6.2 Relationship Between Indoor Radon Concentration and Ventilation Rate

6.2.1 Analysis. Because both the radon entry rate from soil and the air-exchange rate vary with pressure differences across the building shell, the variation of indoor radon concentration with air-exchange rate is more complex than suggested by the simple model introduced in Chapter 1, Section 2.2. An understanding of this relationship is essential for the proper interpretation of indoor concentration measurements, as well as for predicting the change in indoor radon concentration for a specified change in the air-exchange rate. The present state of knowledge is not sufficient to address all possible situations. Consequently, the discussion in this section is illustrative rather than comprehensive.

It is convenient to divide the radon entry modes into two categories. We designate as "passive" those modes that act independently of the pressure difference across the building shell. Specific examples of passive entry are molecular diffusion from building materials (see Chapter 3) and release associated with household water use (see Chapter 4). By contrast, modes that are limited by the rate of pressure-driven flow through the building substructure are designated as "active" entry mechanisms. High rates of radon entry from soil into residential basements are largely due to active modes. The total radon entry rate may be written as the sum of contributions from these two modes:

$$S_v = S_p + S_a(\Delta P_f) \tag{36}$$

where ΔP_f denotes the effective outdoor-indoor pressure difference across the lower part of the building structure.

It is likewise useful to distinguish two ventilation modes. In "balanced" systems the air-exchange rate is effectively independent of the pressure difference across the building shell. A mechanical ventilation system that provides equal supply and exhaust flows is balanced. Infiltration and mechanical ventilation that provides only supply or exhaust are considered "unbalanced" ventilation modes: the air-exchange rate varies directly with the pressure difference across the building shell. The total ventilation rate is the sum of the rates due to these two modes:

$$\lambda_v = \lambda_{v,b} + \lambda_{v,u}(\Delta P) \tag{37}$$

where ΔP is a characteristic pressure difference, such as the mean of the absolute value, across the building envelope.

The unbalanced ventilation component is related to the average pressure difference across the building shell by a power-law relationship (105):

$$\lambda_{v,u} = \frac{E}{V}(\Delta P)^n \qquad 0.5 < n < 1.0 \tag{38}$$

where E is the permeability coefficient of the building envelope (with dimensions $L^{3+n}T^{2n-1}M^{-n}$) and V is the interior volume. E is equal to the product $A_o(2/\rho)^n$, where A_o is the effective leakage area of the envelope (105).

The characteristic pressure difference can be estimated as the sum of three components—those due to temperature differences, wind, and unbalanced mechanical ventilation. (Flow from a chimney would be considered in the last of these categories.)

$$\Delta P = (\rho/2) f_s^2 \left| T_o - T_i \right| + (\rho/2) f_w^2 v^2 + \left| \Delta P_{mv,u} \right| \tag{39}$$

where ρ is the air density, and f_s and f_w are stack and wind parameters (see Chapter 1, Section 8.2 and Ref. 105).

The value of the exponent in Equation 38 is determined by the relative importance of two energy-loss mechanisms as air flows through the penetrations in the building shell. For penetrations that have relatively large width and short length, energy loss is largely due to the inertia of the air at the outlet of the crack. If this is the dominant situation for the structure, the value of the exponent approaches 0.5 for reasons that are analogous to the square-root dependence of the pressure difference with wind speed (see Equation 30). The other limiting case is fully developed laminar flow in the cracks. This case occurs if the cracks are long and narrow and if the flow has a small Reynolds number. In this case, viscous dissipation is the dominant energy loss mechanism. This flow regime is analogous to the flow through soil described by Darcy's law (Equation 20); the exponent in Equation 38 approaches 1.0 in the limit in which this mode dominates. Measurements of n yield values in the range 0.5–0.75 (106, 107). The value $n = 0.5$ has been adopted in a commonly used infiltration model (105).

The variation of the active component of the radon entry rate with pressure difference depends on both the mode of entry and the details of the building-soil air coupling. To be specific, we consider the common example of a house with a basement that has a perimeter penetration such as a crack at the floor-wall joint or a drain tile connected through an untrapped pipe to a basement sump (see also Chapter 10). For small source rates, the concentration of radon in the entering soil gas is independent of the flow rate and, consequently, independent of pressure difference. In this case, assuming that the effective pressure at the base of one or more of the walls is inward (i.e., ΔP_f is positive), $S_a \propto (\Delta P_f)$. On the other hand, if the source rate is large, the soil gas is depleted, and the influence of changes in pressure difference on radon entry is diminished. A theoretical analysis of this situation has shown that $S_a \propto (\Delta P_f)^{0.66}$ in this case, again assuming $\Delta P_f > 0$ (108). If ΔP_f is negative, i.e., the pressure across the building substructure is outward, we expect $S_a \cong 0$. These conditions are summarized by

$$S_a = \begin{cases} 0, & \Delta P_f < 0 \\ \beta(\Delta P_f)^m & \Delta P_f > 0, \quad 0.66 < m < 1.0 \end{cases} \tag{40}$$

where the coefficient β depends on the radium content and emanation coefficient of the soil, on the permeability of the soil, and on the coupling between the building interior and the soil air.

In analogy with Equation 39, ΔP_f can be expressed as the sum of three components (109):

$$\Delta P_f = \rho g(z - z_o)\frac{T_o - T_i}{T_o} + c_f\rho\frac{v^2}{2} + \Delta P_{mv,u} \tag{41}$$

where the thermal effect is an approximation of Equation 35 and c_f is an average pressure coefficient for the lower part of the structure (cf. Equation 31).

We may now write a general expression for the indoor radon concentration for this case. We may rewrite Equation 1 from Chapter 1 as

$$I - I_o = S_v/\lambda_v \tag{42}$$

where we have assumed $\lambda_v >> d$, the radon decay constant (denoted λ_{Rn} elsewhere in this chapter). Substituting Equations 36, 40, and 41 for S_v and Equations 37–39 for λ_v, and assuming that $\Delta P_f > 0$, we obtain

$$I - I_o = \frac{S_p + \beta\left(\rho g(z - z_o)\frac{T_o - T_i}{T_o} + c_f\rho\frac{v^2}{2} + \Delta P_{mv,u}\right)^m}{\lambda_{v,b} + \frac{D}{V}\left[\rho\frac{f_s^2}{2}|T_o - T_i| + \rho f_w^2\frac{v^2}{2} + |\Delta P_{mv,u}|\right)^n} \tag{43}$$

It is instructive to consider two limiting cases. In case a, we assume that the active entry rate is zero. In this case, $I - I_o = S_p/\lambda_v$, and we recover the simple result presented in Chapter 1. In case b, we assume first that $S_p = 0$ and $\lambda_{v,b} = 0$. We also assume that the ratios $\Delta T : v^2 : \Delta P_{mv,u}$ remain constant. The latter assumption would hold, for example, if one of the three terms greatly dominated the other two for both ΔP and ΔP_f. In this case, $I - I_o \propto (\Delta P)^{m-n}$. And, since $\lambda_v \propto (\Delta P)^n$, we obtain the result

$$I - I_o \propto \lambda_v^{[(m-n)/n]} \tag{44}$$

These results are presented in Figure 2.11. For much of case b, the indoor radon concentration is expected to increase with ventilation rate. Note, however, that many assumptions went into this analysis. For example, we implicitly assumed that a single pressure difference ΔP_f could be used to represent the entire base of the building. Although this is reasonable for the thermal and unbalanced mechanical ventilation components, wind pressures are highly directional. A more thorough analysis would treat the walls separately. In addition, the assumption that the pressures due to thermal effects, wind, and unbalanced ventilation remain in con-

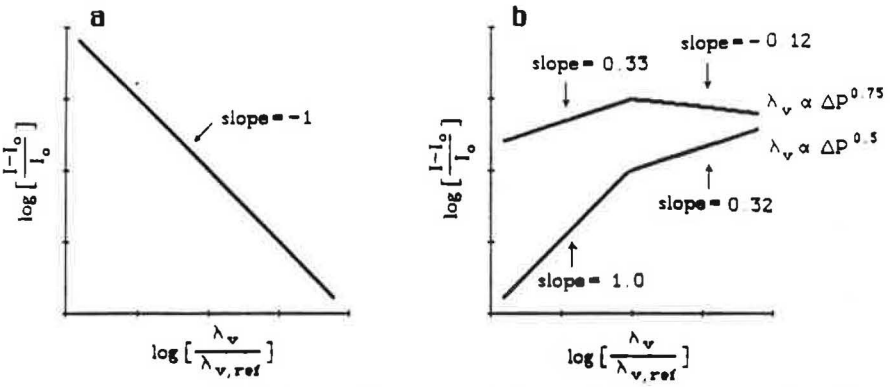

Figure 2.11. Relationship between radon concentration and air-exchange rate for a single structure. In case *a* it is assumed that either the ventilation system is entirely balanced or the radon entry mode is entirely passive. Case *b* represents the other extreme: the entry mode is active and the ventilation mode is unbalanced. In addition, the relative contributions of temperature difference, wind, and mechanical ventilation to the pressure difference are assumed to remain constant for case *b*. $\lambda_{v,ref}$ is an arbitrary, constant air-exchange rate.

stant proportion limits the applicability of this result. Mowris, in analyzing the effect of adding exhaust ventilation to houses, found consistent reduction of indoor radon concentration (109). In any case, it is clear that the relationship between indoor radon concentration and air-exchange rate is a complex one that varies considerably with the particular circumstances of a house.

6.2.2 Experimental Results. The relationship between indoor radon concentration and air-exchange rate in a single house has been examined in detail in two studies. In the first, the ventilation rate in a house with a very low infiltration rate ($<0.1\ h^{-1}$) was varied by means of a balanced mechanical ventilation system (110). As expected, the radon concentration varied as predicted by Equation 42.

In the second study, indoor radon concentration and air-exchange rate were monitored continuously in a house with a basement over a 5-month period (2). In this case, the changes in air-exchange rate were due to a combination of changing weather conditions, the intermittent use of a fireplace and exhaust fans, and the opening of doors and windows. A confounding feature of this experiment in the present context was the bimodal nature of the radon entry rate. It appeared that major pathways for radon entry could be either opened or closed, perhaps owing to changing moisture levels in the nearby soil.

The variation of radon concentration with air-exchange rate from this study is presented in Figure 2.12. In the case of high entry rate (open triangles), the variation is similar to the prediction of Equation 44 with $n = 0.75$ (cf. Fig. 2.11b). For the low-entry-rate case, the behavior is more complex, perhaps indicating that neither passive or active entry modes are dominant.

The curves plotted in Figure 2.12 reflect the predictions of two models. The

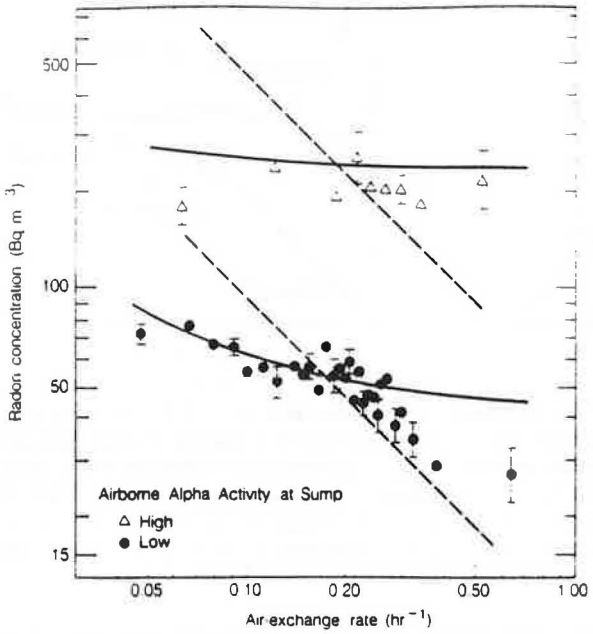

Figure 2.12. Scatter plot of ^{222}Rn concentration versus air-exchange rate averaged over three-hour periods. Measurements were made continuously at a house with a basement in Chicago over a 5-month period. Data were sorted into two groups according to radon concentration above a sump in the basement: the concentration at this point during the "high" periods averaged greater than 10,000 Bq m^{-3}; for "low" periods the average was less than 500 Bq m^{-3}. Each data point gives the geometric mean radon concentration of 19–21 measurements that have been grouped according to air-exchange rate. Error bars represent one geometric standard deviation of the mean. The dashed lines represent the expected relationship if the radon entry rate is independent of air-exchange rate. The solid lines reflect a model in which radon entry is presumed to have two components—one (diffusive) being constant, the other (convective) being proportional to air-exchange rate. Reproduced from Ref. 2.

dashed line corresponds to Equation 42 with $I >> I_o$. The solid line reflects a simplified two-component entry model. In particular, the active entry component is assumed to be proportional to the infiltration rate. This would be expected if the exponent in Equation 38 was $n = 1$, and if the source rate was small. D'Ottavio and Dietz showed, by extending the formulation of this model to incorporate radon entering from outdoor air and the variability of radon concentration in soil air, that a better fit to a portion of the data could be obtained (111).

6.3 Modeling Radon Entry

The complexities associated with the production and migration of radon in soil, and its entry into buildings point to the need for detailed mathematical models to develop a complete understanding of the effects of the many factors involved. The

development of such a model has been undertaken (7, 75–77). In this work, a finite-element approach is used, with the soil comprising 1780 variable-sized elements. The model has thus far been restricted to examining uniform and isotropic soils, houses with basements, radon transport due to convective flow, and pressure gradients arising from temperature differences and wind. Nevertheless, some interesting and useful results have been obtained: for one case, an increase in permeability from 10^{-11} to 10^{-10} m^2 led to an increase in radon entry rate by a factor of 4.5 (7); variations in wind speed and direction can lead to substantial changes in radon entry rate in the absence of other factors (77); for a typical Canadian house with surrounding soil having a radium content of 59 Bq kg^{-1} and permeability 5 $\times$ 10^{-11} m^2, the average radon entry rate and radon concentration would be 4 $\times$ 10^7 Bq h^{-1}, and approximately 200 Bq m^{-3}, respectively (77).

Recently, a finite difference model and a simplified analytical model were developed for computing soil gas entry rates into crawl space and basement houses (109, 120). The models have been used to examine the effect of exhaust ventilation on radon entry rates and indoor concentrations. They clearly have broader application.

Loureiro has developed perhaps the most general model of radon entry to date (121). Based again on a finite-difference method, the model simulates radon migration by both diffusion and convection in the vicinity of a basement having a floor-wall gap. An aggregate layer adjacent to the basement may be specified to have distinct characteristics from the remainder of the soil.

7 GEOGRAPHICAL CHARACTERIZATION

The importance of soil as a source of indoor radon, combined with the increasing evidence of unacceptably high radon concentrations in a significant fraction of houses, has raised the question of whether one might predict on a geographical basis where high indoor radon levels are likely to be found. If a method to achieve this were developed and validated, the cost of identifying houses with elevated levels could be considerably reduced. The case that such an effort could succeed is strengthened by the direct observation that there is a substantial variance in the mean indoor radon concentration among different areas (8). (See also Chapters 1 and 12, especially Figure 12.4.)

Several pertinent sources of information may be useful in a geographical characterization effort. From the discussion in this chapter, we may say that the potential for high radon entry rates depends on several factors: the radium content of the soil; the temporal state of the soil, particularly its moisture content; the soil permeability; and the weather—particularly temperature, wind, and rainfall. In the United States, information on these variables is available from the Department of Energy's National Uranium Resource Evaluation program (results distributed by the U.S. Geological Survey), the Department of Agriculture's Soil Conservation Service reports, and the Department of Commerce's National Climatic Center reports. The present state of knowledge concerning the relevance of these data to

estimating radon source potential on a geographical basis is reported in a recent paper (112).

An important factor that is not completely understood is the extent to which some of these parameters vary over relevant spatial scales. The uncertainty is most evident with respect to permeability, which, because of the broad range of values it may have, is perhaps the most important of the determining variables. For geographical characterization to be useful, variations in permeability over a scale at least as large as a substantial fraction of a community must be of a comparable size to variations on a house-to-house basis.

One approach to geographical characterization that has been proposed is the development of a radon index number (RIN) that would combine the major factors determining radon entry into a single variable (76, 77). The proposed formulations have considered weather effects to be constant for a given area and, hence, do not incorporate them into the RIN. Building ventilation rates have been explicitly incorporated into one proposal, however. The two forms are given below.

$$\text{RIN} = \frac{hA_{Ra}}{-\log k} \tag{45}$$

where h is the inverse average air-exchange rate, A_{Ra} is the radium activity concentration of the soil, and k is the permeability (76).

$$\text{RIN} = \log A_{Ra} + 0.45 \log k \tag{46}$$

where the factor 0.45 was based on numerical modeling of radon entry as previously described (77).

Several other studies have addressed the topic of geographical characterization. In Sweden, "GEO-radiation" maps have been produced from airborne radiometric surveys, ground measurements of gamma radiation, and geological mapping (113, 114). The purpose of these maps is to document areas and rock types with gamma emission levels exceeding 7.7×10^{-9} C kg^{-1} h^{-1} (30 μR h^{-1}), with the intention of identifying areas at risk for high indoor radon levels due to entry from soil. Kothari and Han (115) have shown a correlation for nine U.S. communities between the geometric mean indoor radon concentration and the geometric mean equivalent uranium (eU) concentration of the soil, as determined from an aerial radiometric survey. Figure 2.13, based on their results, shows that the order-of-magnitude range in eU is associated with roughly a factor-of-five range in indoor radon concentrations. Moed et al. (40) examined the aerial radiometric data from the NURE program for the western U.S., and produced the map of surface ^{226}Ra concentrations shown in Figure 2.5. They also showed that the variations in the aerial data corresponded to differences in radium content, radon flux, and gamma emission rate measured at the ground. Duval (116) has developed a technique of producing composite color images from the NURE data that may prove to be a useful tool in geographical characterization of radon source potential.

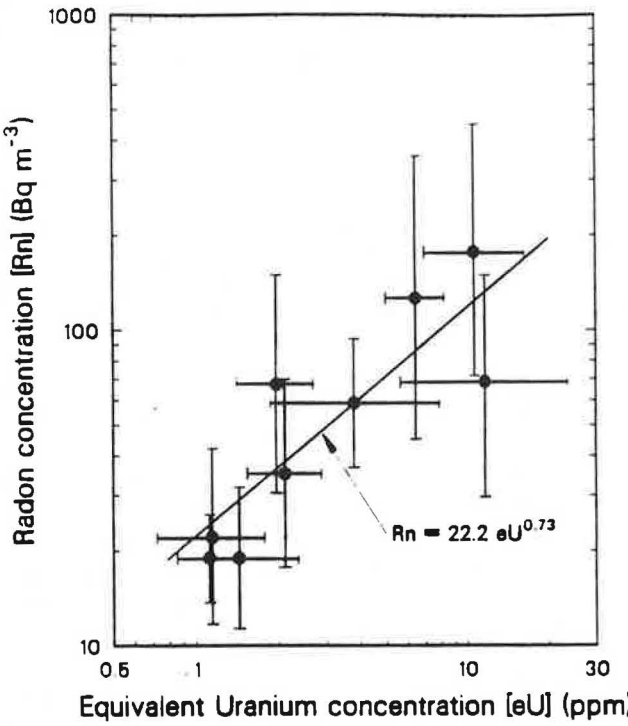

Figure 2.13. Scatter plot of geometric mean indoor ^{222}Rn concentration and soil equivalent uranium concentration for nine U.S. communities. Error bars indicate one geometric standard deviation. Each point represents radon measurements in 8–69 houses. Equivalent uranium concentration was determined from an analysis of airborne radiometric (NARR) data. 1 ppm equivalent uranium equals 12.4 Bq kg^{-1}. Data from Ref. 115.

8 CONCLUSIONS

Within the past decade the consensus concerning the nature and extent of the problem of radon in indoor air has been radically revised. Rather than being a problem that arises due to molecular diffusion of radon from industrially contaminated building materials or fill materials, we now recognize that the vast majority of structures with elevated indoor concentrations are unexceptional in other regards. In most cases, radon enters predominantly via the substructure through the combined effects of molecular diffusion and convective flow. The importance of the convective flow process is seen in the considerable success of control measures directed at blocking entry pathways or reversing the ordinary direction of flow, as discussed in Chapter 10.

Despite our considerable progress, much work remains before we can, first, confidently assert that we understand the sources of indoor radon and, second, fully exploit that understanding in reducing exposures. Key areas requiring further work include continued development of numerical models of the process of radon

migration in soil, studies of the multiple roles of moisture in affecting radon emanation and transport, and investigations of the usefulness of various data, particularly those relating to permeability, in predicting radon entry rate potential.

REFERENCES

1. George, A. C., and Breslin, A. J. (1980). The distribution of ambient radon and radon daughters in residential buildings in the New Jersey–New York area. In T. F., Gesell, and W. M. Lowder (eds.), *Proc. Natural Radiation Environment III*, Conf-780422, U.S. Dept. of Commerce, National Technical Information Service, Springfield, VA p. 1272.
2. Nazaroff, W. W., Feustel, H., Nero, A. V., Revzan, K. L. Grimsrud, D. T., Essling, M. A., and Toohey, R. E. (1985). Radon transport into a detached one-story house with a basement, *Atmos. Environ.*, **19**, 31.
3. *Proc. Third Workshop on Radon and Radon Daughters Associated with Uranium Mining and Processing* (1980). Atomic Energy Control Board, Ottawa, Canada.
4. Ericson, S. O., and Schmied, H. (1984). Modified technology in new constructions, and cost effective remedial action in existing structures, to prevent infiltration of soil gas carrying radon. In B. Berglund, T. Lindvall, and J. Sundell (eds.), *Indoor Air: Buildings, Ventilation and Thermal Climate*, vol. 5, Swedish Council for Building Research, Stockholm, p. 153.
5. Nitschke, I. A., Wadach, J. B., Clarke, W. A., Traynor, G. W., Adams, G. P., and Rizzuto, J. E. (1984). A detailed study of inexpensive radon control techniques in New York State houses. In B. Berglund, T. Lindvall, and J. Sundell (eds.), *Indoor Air: Buildings, Ventilation and Thermal Climate*, vol. 5, Swedish Council for Building Research, Stockholm, p. 111.
6. Bruno, R. C. (1983). Sources of indoor radon in houses: A review, *J. Air Pollut. Contr. Assoc.*, **33**, 105.
7. DSMA Atcon, Ltd. (1983). Review of existing instrumentation and evaluation of possibilities for research and development of instrumentation to determine future levels of radon at a proposed building site, report INFO-0096, Atomic Energy Control Board, Ottawa.
8. Nero, A. V., Schwehr, M. B., Nazaroff, W. W., and Revzan, K. L. (1986). Distribution of airborne radon-222 concentrations in U.S. homes, *Science*, **234**, 992.
9. Scott, R. F., (1963). *Principles of Soil Mechanics*, Addison-Wesley, Reading, MA.
10. Terzaghi, K., and Peck, R. B. (1967). *Soil Mechanics in Engineering Practice*, 2nd ed., Wiley, New York.
11. Baver, L. D. (1940). *Soil Physics*, Wiley, New York.
12. Scheidegger, A. E. (1960). *The Physics of Flow Through Porous Media*, 2nd ed., Macmillan, New York.
13. Muskat, M. (1946). *The Flow of Homogeneous Fluids Through Porous Media*, Edwards, Ann Arbor, MI.
14. Collins, R. E. (1961). *Flow of Fluids Through Porous Materials*, Reinhold, New York.

15. *Symp. on Flow Through Porous Media* (1969). American Chemical Society Publications, Washington, DC.
16. Childs, E. C. (1969). *An Introduction to the Physical Basis of Soil Water Phenomena*, Wiley, London.
17. Marshall, T. J. and Holmes, J. W. (1979). *Soil Physics*, Cambridge University Press, London, p. 12.
18. Corey, A. T. (1957). Measurement of water and air permeability in unsaturated soil, *Soil Sci. Soc. Am. Proc.*, **21**, 7.
19. Botset, H. G. (1940). Flow of gas-liquid mixtures through consolidated sand, *Am. Inst. Mining Eng. Trans.*, **136**, 91.
20. Osaba, J. S., Richardson, J. G., Kerver, J. K., Hafford, J. A., and Blair, P. M. (1951). Laboratory measurements of relative permeability, *Am. Inst. Mining Eng. Trans.*, **192**, 47.
21. Mitchell, T. K., Hooper, D. R., and Campanella, R. G. (1965). Permeability of compacted clay, *Am. Soc. Civil Eng. Proc.*, **SM4**, 41.
22. Barden, L., and Pavlakis, G. (1971). Air and water permeability of compacted unsaturated cohesive soil, *J. Soil Sci.*, **22**, 302.
23. Garcia-Bengochea, I., Lovell, C. W., and Altschaeffl, A. G. (1979). Pore distribution and permeability of silty clays, *Proc. ASCE*, **105**, 839.
24. Rice, P. A., Fontugne, D. J., Latini, R. G., and Barduhn, A. J. (1969). Anisotropic permeability in porous media. In *Symp. on Flow Through Porous Media*, American Chemical Society Publications, Washington, DC. p. 48.
25. Bowles, J. E. (1979). *Physical and Geotechnical Properties of Soils*, McGraw-Hill, New York, p. 213.
26. Topp, G. C., Zabcuk, W. D., and Dumanski, J. (1980). The variation of in-situ measured soil water properties within soil map units, *Can J. Soil Sci.*, **60**, 497.
27. McKeague, J. A., Wang, C., and Topp, G. C. (1982). Estimating saturated hydraulic conductivity from soil morphology, *Soil Sci. Soc. Am. J.*, **46**, 1239.
28. Wilkening, M. H., Clements, W. E., and Stanley, D. (1972). Radon-222 flux measurements in widely separated regions. In J. A. S. Adams, W. M. Lowder, and T. F. Gesell (eds.), *Proc. Natural Radiation Environment II*, Conf-720805, U.S. Dept. of Commerce, National Technical Information Service, Springfield, VA, p. 717.
29. Pearson, J. E., and Jones, G. E. (1965). Emanation of radon 222 from soils and its use as a tracer, *J. Geophys. Res.*, **70**, 5279.
30. Fleischer, R. L., and Mogro-Campero, A. (1980). Techniques and principles for mapping integrated radon emanation within the earth. In T. F. Gesell and W. M. Lowder (eds.), *Natural Radiation Environment III*, Conf-780422, U.S. Dept. of Commerce, National Technical Information Service, Springfield, VA, p. 57.
31. Silker, W. B., and Kalkwarf, D. R. (1983). Radon diffusion in candidate soils for covering uranium mill tailings, report NUREG/CR-2924, PNL-4434, Pacific Northwest Laboratory, Richland, WA.
32. Strong, K. P., Levins, D. M., and Fane, A. G. (1981). Radon diffusion through uranium tailings and earth cover. In M. Gomez (ed.), *Radiation Hazards in Mining: Control, Measurement and Medical Aspects*, Society of Mining Engineers, New York, p. 713.

33. King, C. Y. (ed.) (1984/1985). Earthquake hydrology and chemistry, special issue of *J. Appl. Geophys.*, **122**, 294.

34. Hirst, W. and Harrison, G. E., (1939). The diffusion of radon gas mixtures, *Proc. Roy. Soc. London (A)*, **169**, 573.

35. Buckingham, E. (1904). Contributions to our knowledge of the aeration of soils, bulletin No. 25, US Dept. of Agriculture, Bureau of Soils, Washington, DC.

36. Penman, H. L. (1940). Gas and vapour movements in soil: The diffusion of vapours through porous solid, *J. Agr. Sci.*, **30**, 437.

37. Currie, J. A. (1960). Gaseous diffusion in porous media. Part 2—Dry granular materials, *Br. J. Appl. Phys.*, **11**, 318.

38. Tanner, A. B. (1964). Radon migration in the ground: A review, In J. A. S. Adams and W. M. Lowder (eds.), *Natural Radiation Environment*, University of Chicago Press, Chicago, p. 161.

39. Currie, J. A. (1961). Gaseous diffusion in porous media. Part 3—Wet granular materials, *Br. J. Appl. Phys.*, **12**, 275.

40. Moed, B. A., Nazaroff, W. W., Nero, A. V., Schwehr, M. B., and Van Heuvelen, A. (1984). Identifying areas with potential for high indoor radon levels: Analysis of the National Airborne Radiometric Reconnaissance Data for California and the Pacific Northwest, report LBL-16955, Lawrence Berkeley Laboratory, Berkeley, CA.

41. Kirkegaard, P., and Lovborg, L. (1980). Transport of terrestrial gamma radiation in plane semi-infinite geometry, *J. Comp. Phys.*, **36**, 20.

42. Myrick, T. E., Berven, B. A., and Haywood, F. F. (1983). Determination of concentrations of selected radionuclides in surface soil in the U.S., *Health Phys.*, **45**, 631.

43. Wollenberg, H. A. (1984). Naturally occurring radioelements and terrestrial gamma-ray exposure rates: An assessment based on recent geochemical data, report LBL-18714, Lawrence Berkeley Laboratory, Berkeley, CA.

44. Powers, R. P., Turnage, N. E., and Kanipe, L. G. (1980). Determination of radium-226 in environmental samples. In T. F. Gesell and W. M. Lowder (eds.), *Natural Radiation Environment III*, Conf-780422, US Dept. of Commerce, National Technical Information Service, Springfield, VA, p. 640.

45. Iyengar, M. A. R., and Markose, P. M. (1982). An investigation into the distribution of uranium and daughters in the environment of a uranium ore processing facility. Cited in Raghavayya, M., Khan, A. H., Padmanabhan, N., and Srivastava, G. K., Exhalation of Rn-222 from soil: Some aspects of variation. In K. G. Vohra, U. C. Mishra, K. C. Pillai, and S. Sadasivan (eds.), *Natural Radiation Environment*, Wiley Eastern, New Delhi, p. 584.

46. Kalin, M., and Sharma, H. D. (1981). Radium-226 and other group two elements in abandoned uranium mill tailings in two mining areas in south central Ontario. In M. Gomez (ed.), *Radiation Hazards in Mining: Control, Measurement and Medical Aspects*, Society of Mining Engineers, New York, p. 707.

47. Bossus, D. A. W. (1984). Emanating power and specific surface area, *Radiat. Prot. Dosim.*, **7**, 73.

48. Tanner, A. B. (1980). Radon migration in the ground: a supplementary review. In T. F. Gesell and W. M. Lowder (eds.), *Proc. Natural Radiation Environment III*, Conf-780422, US Dept. of Commerce, National Technical Information Service, Springfield, VA, p. 5.

49. Andrews, J. N., and Wood, D. F. (1972). Mechanism of radon release in rock matrices and entry into groundwaters, *Trans. Inst. Min. Metall. Sec. B*, **81**, 198.

50. Megumi, K., and Mamuro, T. (1974). Emanation and exhalation of radon and thoron gases from soil particles, *J. Geophys. Res.*, **79**, 3357.

51. Jasinska, M., Niewiadomski, T., and Schwabenthan, J. (1982). Correlation between soil parameters and natural radioactivity. In K. G. Vohra, U. C. Mishra, K. C. Pillai, and S. Sadasivan (eds.), *Natural Radiation Environment*, Wiley Eastern, New Delhi, p. 206.

52. Barretto, P. M. C., (1973). Emanation characteristics of terrestrial and lunar materials and the radon-222 loss effect on the uranium-lead system discordance, Ph.D. thesis, Rice University, Houston.

53. Wilkening, M. H. (1974). Radon-222 from the island of Hawaii: Deep soils are more important than lava fields or volcanoes, *Science*, **183**, 413.

54. Thamer, B. J., Nielson, K. K., and Felthauser, K. (1981). The effects of moisture on radon emanation including the effects on diffusion, report BuMines OFR 184-82, PB83-136358, US Dept. of Commerce, National Technical Information Service, Springfield, VA.

55. Strong, K. P., and Levins, D. M. (1982). Effect of moisture content on radon emanation from uranium ore and tailings, *Health Phys.*, **42**, 27.

56. Stranden, E., Kolstad, A. K., and Lind, B. (1984). The influence of moisture and temperature on radon exhalation, *Radiat. Prot. Dosim*, **7**, 55.

57. Ingersoll, J. G. (1983). A survey of radionuclide contents and radon emanation rates in building materials used in the U.S., *Health Phys.*, **45**, 363.

58. Bird, R. B., Stewart, W. E., and Lightfoot, E. N. (1960). *Transport Phenomena*, Wiley, New York.

59. Tanner, A. B. (1985). US Geological Survey National Center, Reston, VA, personal communication.

60. Gray, R. W., and Ramsay, W. (1909). Some physical properties of radium emanation, *J. Chem. Soc. (London) Trans.*, **95**, 1073.

61. Rutherford, E., and Soddy, F. (1903). Condensation of radioactive emanations, *Phil. Mag. Ser. 6*, **5**, 561.

62. Lucas, H. F. (1957). Improved low-level alpha scintillation counter for radon, *Rev. Sci. Instrum.*, **28**, 680.

63. Ingersoll, J. G., Stitt, B. D., and Zapalac, G. H. (1983). A fast and accurate method for measuring radon exhalation rates from building materials, *Health Phys.*, **45**, 550.

64. Nazaroff, W. W., and Doyle, S. M. (1985). Radon entry into houses having a crawl space, *Health Phys.*, **48**, 265.

65. Liddament, M., and Allen, C. (1983). The validation and comparison of mathematical models of air infiltration, technical note AIC-11, Air Infiltration Centre, Berkshire, England.

66. Fisk, W. J., and Turiel, I. (1983). Residential air-to-air heat exchangers: Performance, energy savings and economics, *Energy and Buildings*, **5**, 197.

67. Modera, M. P., and Sonderegger, R. C. (1980). Determination of the *in-situ* performance of fireplaces, report LBL-10701, Lawrence Berkeley Laboratory, Berkeley, CA.

68. Hernandez, T. L., and Ring, J. W. (1982). Indoor radon source fluxes: experimental tests of a two-chamber model. *Environ. Int.*, **8**, 45.

69. Hernandez, T. L., Ring, J. W., and Sachs, H. (1984). The variation of basement radon concentration with barometric pressure. *Health Phys.*, **46**, 440.

70. Holub, R. F., Droullard, R. F., Borak, T. B., Inkret, W. C., Morse, J. G., and Baxter, J. F. (1985). Radon-222 and ^{222}Rn progeny concentrations in an energy-efficient house equipped with a heat exchanger. *Health Phys.*, **49**, 267.

71. Scott, A. G., and Findlay, W. O. (1983). Demonstration of remedial techniques against radon in houses on Florida phosphate lands, report EPA 520/5-83-009, US Environmental Protection Agency, Eastern Environmental Radiation Facility, Montgomery, AL.

72. Crane, T. (1947). *Architectural Construction: The Choice of Membrane Materials*, Wiley, New York.

73. *Uniform Building Code* (1982). International Conference of Building Officials, Whittier, CA.

74. Rundo, J., Markun, F., and Plondke, N. J. (1979). Observation of high concentrations of radon in certain houses. *Health Phys.*, **36**, 729.

75. Scott, A. G. (1983). Computer modelling of radon movement. In A. C. George, W. Lowder, I. Fisenne, E. O. Knutson, and L. Hinchcliffe (eds.), *EML Indoor Radon Workshop, 1982*, report EML-416, Environmental Measurements Laboratory, New York, p. 82.

76. Eaton, R. S., and Scott, A. G. (1984). Understanding radon transport into houses. *Radiat. Prot. Dosim.* **7**, 251.

77. DSMA Atcon, Ltd. (1985). A computer study of soil gas movement into buildings, report 1389/1333, Department of Health and Welfare, Ottawa.

78. Youngquist, G. R. (1969). Diffusion and flow of gases in porous solids. In *Symp. on Flow Through Porous Media*, American Chemical Society Publications, Washington, DC, p. 58.

79. Boyle, R. W. (1911). The solubility of radium emanation. Application of Henry's law at low partial pressures. *Phil. Mag.*, **22**, 840.

80. Crozier, W. D. (1969). Direct measurements of radon-220 (thoron) exhalation from the ground. *J. Geophys. Res.*, **74**, 4199.

81. Culot, M. V. J., Olson, H. G., and Schiager, K. J. (1976). Effective diffusion coefficient of radon in concrete, theory and method for field measurements. *Health Phys.*, **30**, 263.

82. Collé, R., Rubin, R. J., Knab, L. I., and Hutchinson, J. M. R. (1981). Radon transport through and exhalation from building materials: A review and assessment, NBS technical note 1139, US Government Printing Office, Washington, DC.

83. Landman, K. A. (1982). Diffusion of radon through cracks in a concrete slab. *Health Phys.*, **43**, 65.

84. Landman, K. A., and Cohen, D. S. (1983). Transport of radon through cracks in a concrete slab. *Health Phys.*, **44**, 249.

85. Nero, A. V., and Nazaroff, W. W. (1984). Characterising the source of radon indoors. *Radiat. Prot. Dosim.*, **7**, 23.

86. Burmister, D. M. (1954). Principles of permeability testing of soils. In *Symp. on Permeability of Soils*, ASTM Special Technical Publication no. 163, American Society for Testing Materials, Philadelphia, p. 3.

107. Modera, M. P., Sherman, M. H., and Levin, P. A., (1983). A detailed examination of the LBL infiltration model using the mobile infiltration test unit, report LBL-15636, Lawrence Berkeley Laboratory, Berkeley, CA.

108. Nazaroff, W. W., and Sextro, R. G. (1987). Analysis of a technique for measuring the indoor radon-222 source potential of soil, submitted to *Environ. Sci. Technol.*

109. Mowris, R. J. (1986). Analytical and numerical models for estimating the effect of exhaust ventilation on radon entry in houses with basements or crawl spaces, M.S. thesis, University of Colorado (also issued as report LBL-22067, Lawrence Berkeley Laboratory, Berkeley, CA).

110. Nazaroff, W. W., Boegel, M. L., Hollowell, C. D., and Roseme, G. D. (1981). The use of mechanical ventilation with heat recovery for controlling radon and radon-daughter concentrations in houses, *Atmos. Environ.*, **15**, 263.

111. D'Ottavio, T. W., and Dietz, R. N. (1986). Discussion of 'Radon transport into a detached one-story house with a basement', *Atmos. Environ.*, **20**, 1065.

112. Nazaroff, W. W., Moed, B. A., Sextro, R. G., Revzan, K. L., and Nero, A. V. (1987). Factors influencing soil as a source of indoor radon: A framework for geographically assessing radon source potentials, report LBL-20645, Lawrence Berkeley Laboratory, Berkeley, CA.

113. Åkerblom, G., and Wilson, C. (1982). Radon—Geological aspects of an environmental problem, rapporter och meddalanden nr 30, Sveriges Geologiska Undersökning, Luleå, Sweden.

114. Wilson, C. (1984). Mapping the radon risk of our environment. In B. Berglund, T. Lindvall, and J. Sundell (eds.), *Indoor Air: Radon, Passive Smoking, Particulates and Housing Epidemiology*, vol. 2, Swedish Council for Building Research, Stockholm, p. 85.

115. Kothari, B. K., and Han, Y. (1984). Association of indoor radon concentrations with airborne surveys of uranium in surficial material, *Northeastern Environ. Sci.*, **3**, 30.

116. Duval, J. S. (1983). Composite color images of aerial gamma-ray spectrometric data, *Geophysics*, **48**, 722.

117. Marshall, T. J. (1985), A relation between permeability and size distribution of soil pores, *J. Soil Sci.*, **9**, 1.

118. Sisigina, T. I. (1974). Assessment of radon emanation from the surface of extensive territories. In *Nuclear Meteorology*, Israeli Program of Scientific Translations, Jerusalem, p. 239.

119. Damkjær, A., and Korsbech, U. (1985). Measurement of the emanation of radon-222 from Danish soils, *Sci. Total Environ.*, **45**, 343.

120. Mowris, R. J., and Fisk, W. J. (1987). Modeling the effects of exhaust ventilation on radon entry rates and indoor radon concentrations, report LBL-22939, Lawrence Berkeley Laboratory, Berkeley, CA, submitted to *Health Phys.*

121. Loureiro, C. (1987). Simulation of the steady-state transport of radon from soil into houses with basements under constant negative pressure, Ph.D. Thesis, University of Michigan, Ann Arbor.

87. Schlichting, H. (1979). *Boundary-Layer Theory*, 7th ed., McGraw-Hill, New York.

88. Whitaker, S. (1984). *Introduction to Fluid Mechanics*, reprint ed., R. E. Krieger Publishing Co., Malabar, FL.

89. Lorrain, P., and Corson, D. (1970). *Electromagnetic Fields and Waves*, 2nd ed., Freeman, San Francisco, Chap. 2.

90. Carslaw, H. S., and Jaeger, J. C. (1959, reprinted 1984). *Conduction of Heat in Solids*, 2nd ed., Oxford University Press, New York.

91. Morse, P. M., and Feshbach, H. (1953). *Methods of Theoretical Physics*, 2 vol., McGraw-Hill, New York, Chap. 10.

92. Nazaroff, W. W., Lewis, S. R., Doyle, S. M., Moed, B. A., and Nero, A. V. (1987). Experiments on pollutant transport from soil into residential basements by pressure-driven airflow, *Environ. Sci. Technol.*, **21**, 459.

93. Desai, C. S., and Abel, J. F. (1972). *Introduction to the Finite Element Method: A Numerical Method for Engineering Analysis*, Van Nostrand Reinhold, New York.

94. Bates, R. C., and Edwards, J. C. (1981). The effectiveness of overpressure ventilation: a mathematical study. In M. Gomez (ed.), *Radiation Hazards in Mining: Control, Measurement and Medical Aspects*, Society of Mining Engineers, New York, p. 149.

95. Israelsson, S. (1980). Meteorological influences on atmospheric radioactivity and its effects on the electrical environment. In T. F. Gesell and W. M. Lowder (eds.), *Natural Radiation Environment III*, Conf-780422, US Dept. of Commerce, National Technical Information Service, Springfield, VA, p. 210.

96. Kraner, H. W., Schroeder, G. L., and Evans, R. D. (1964). Measurements of the effects of atmospheric variables on radon-222 flux and soil-gas concentrations. In J. A. S. Adams and W. M. Lowder (eds.), *Natural Radiation Environment*, University of Chicago Press, Chicago, p. 191.

97. Rogers, V. C., Nielson, K. K., Merrell, G. B., and Kalkwarf, D. R. (1983). The effects of advection on radon transport through earthen materials, report NUREG/CR-3409, PNL-4789, RAE-18-4, US Nuclear Regulatory Commission, Washington, DC.

98. Clements, W. E., and Wilkening, M. H. (1974). Atmospheric pressure effects on ^{222}Rn transport across the earth-air interface, *J. Geophys. Res.*, **79**, 5025.

99. Schery, S. D., Gaeddert, D. H., and Wilkening, M. H. (1982). Transport of radon from fractured rock, *J. Geophys. Res.*, **87**, 2969.

100. Schery, S. D., Gaeddert, D. H., and Wilkening, M. H. (1984). Factors affecting exhalation of radon from a gravelly sandy loam, *J. Geophys. Res.*, **89**, 7299.

101. Sachs, P. (1972). *Wind Forces in Engineering*, Pergamon Press, Oxford.

102. Simiu, E., and Scanlan, R. H. (1978). *Wind Effects on Structures: An Introduction to Wind Engineering*, Wiley, New York.

103. Fukuda, H. (1955). Air and vapor movement in soil due to wind gustiness, *Soil Sci.*, **79**, 249.

104. Van der Hoven, I. (1957). Power spectrum of horizontal wind speed in the frequency range from 0.0007 to 900 cycles per hour, *J. Meteor.*, **14**, 160.

105. Sherman, M. H. (1980). Air infiltration in buildings, Ph.D. thesis, University of California, Berkeley.

106. Blomsterberg, A. K., Sherman, M. H., and Grimsrud, D. T. (1979). A model correlating air tightness and air infiltration in houses, report LBL-9625, Lawrence Berkeley Laboratory, Berkeley, CA.